Structure and Bonding in the Unsaturated Hydride- and Hydrocarbyl-Bridged Complexes $[Mo_2(\eta^5\text{-}C_5H_5)_2(\mu\text{-}X)(\mu\text{-}PCy_2)(CO)_2]$ (X = H, CH_3, CH_2Ph, Ph). Evidence for the Presence of α-Agostic and π-Bonding Interactions†

M. Esther García,‡ Alberto Ramos,‡ Miguel A. Ruiz,*,‡ Maurizio Lanfranchi,§ and Luciano Marchio§

Departamento de Química Orgánica e Inorgánica/IUQOEM, Universidad de Oviedo, 33071 Oviedo, Spain, and Dipartimento di Chimica Generale ed Inorganica, Chimica Analitica, Chimica Fisica, Università di Parma, Parco Area delle Science 17/A, I-43100 Parma, Italy

Received July 19, 2007

The reactions of the triply bonded anion $[Mo_2Cp_2(\mu\text{-}PCy_2)(\mu\text{-}CO)_2]^-$ (Li^+ salt) with $[NH_4]PF_6$, MeI, and $PhCH_2Cl$ give, with good yields, the corresponding hydride- or alkyl-bridged derivatives $[Mo_2Cp_2(\mu\text{-}X)(\mu\text{-}PCy_2)(CO)_2]$ (X = H, Me, CH_2Ph). The related phenyl complex $[Mo_2Cp_2(\mu\text{-}Ph)(\mu\text{-}PCy_2)(CO)_2]$ can be obtained upon reaction of the above anion with Ph_3PbCl. According to the corresponding X-ray diffraction studies, the latter complex displays its phenyl group bonded to the dimetal center exclusively through the ipso carbon atom, while the methyl and benzyl complexes adopt an asymmetric α-agostic structure whereby one of the C−H bonds of the bridgehead carbon is bound to one of the molybdenum atoms. The intermetallic distances remain quite short in all cases, 2.56−2.58 Å. In solution, the hydride complex exhibits dynamic behavior involving mutual exchange of the carbonyl ligands. The alkyl derivatives behave similarly to each other in solution and also exhibit dynamic behavior, possibly implying the presence of small amounts of a nonagostic structure in equilibrium with the dominant α-agostic structure. Density functional theory calculations (B3LYP, B3PW91) correctly reproduce the experimental structures, and predict an α-agostic structure for both the methyl and benzyl complexes. The bonding in the above hydride and hydrocarbyl complexes was analyzed using molecular orbital, atoms in molecules, and natural bond orbital methodologies. The intermetallic binding in the hydride complex can be thus described as composed of a tricentric (Mo_2H) plus two bicentric (Mo_2) interactions, the latter being of σ and π types. In the hydrocarbyl-bridged complexes, analogous tricentric (Mo_2C), and bicentric (Mo_2) interactions can be identified, but there are additional interactions reducing the strength of the intermetallic binding, these being the α-agostic bonding in the case of the alkyl complexes and a π-donor interaction from the π-bonding orbitals of the hydrocarbon ring into suitable metal acceptor orbitals, in the case of the phenyl complex. The strength of these additional interactions have been estimated by second-order perturbation analysis to be of 70.3 (Me), 89.2 (CH_2Ph), and 52.2 (Ph) kJ mol^{-1}, respectively.

Introduction

Recently we reported the preparation of the triply bonded anion $[Mo_2Cp_2(\mu\text{-}PCy_2)(\mu\text{-}CO)_2]^-$, a useful synthetic intermediate exhibiting two different nucleophilic positions located at the metal and the oxygen atoms, which opens the way to several interesting unsaturated derivatives. Thus, the reactions with $[NH_4]PF_6$ and MeI occur at the dimetal center to give the unsaturated hydride $[Mo_2Cp_2(\mu\text{-}H)(\mu\text{-}PCy_2)(CO)_2]$ (**1**) and the methyl derivative $[Mo_2Cp_2(\mu\text{-}Me)(\mu\text{-}PCy_2)(CO)_2]$ (**2**), respectively, while the use of $[Me_3O]BF_4$ as the methylating agent gives the triply bonded methoxycarbyne derivative $[Mo_2Cp_2(\mu\text{-}COMe)(\mu\text{-}PCy_2)(\mu\text{-}CO)]$ instead.[1] The above hydride and methoxycarbyne complexes are very reactive species, and we have studied their chemistry in detail,[2,3] but we were also interested in exploring the chemical behavior of the unsaturated methyl complex **2** and related compounds. Methyl- and other alkyl-bridged complexes are species of interest for several reasons: they serve as models both for intermediates in alkyl-transfer processes and for adsorbates in several heterogeneously catalyzed reactions such as the Fischer−Tropsch synthesis, and they are also implied as catalysts or precursors of the homogeneous catalysts used in the polymerization of olefins.[4,5] Although a large number of such binuclear complexes have been reported so far, only a reduced number of them display metal−metal bonds, and these can be grouped in two structural

† This paper is dedicated to Dr. Antonio Tiripicchio, distinguished professor at the Università di Parma, in recognition of so many years of helpful structural advice and support.

* To whom correspondence should be addressed. E-mail: mara@uniovi.es.
‡ Universidad de Oviedo.
§ Università di Parma.

(1) García, M. E.; Melón, S.; Ramos, A.; Riera, V.; Ruiz, M. A.; Belletti, D.; Graiff, C.; Tiripicchio, A. *Organometallics* **2003**, *22*, 1983.

(2) (a) Alvarez, C. M.; Alvarez, M. A.; García, M. E.; Ramos, A.; Ruiz, M. A.; Lanfranchi, M.; Tiripicchio, A. *Organometallics* **2005**, *24*, 7. (b) Alvarez, M. A.; García, M. E.; Ramos, A.; Ruiz, M. A. *Organometallics* **2006**, *25*, 5374. (c) Alvarez, C. M.; Alvarez, M. A.; García, M. E.; Ramos, A.; Ruiz, M. A.; Graiff, C.; Tiripicchio, A. *Organometallics* **2007**, *26*, 321. (d) Alvarez, M. A.; García, M. E.; Ramos, A.; Ruiz, M. A. *Organometallics* **2007**, *26*, 1461.

(3) Alvarez, C. M.; Alvarez, M. A.; García, M. E.; García-Vivó, D.; Ruiz, M. A. *Organometallics* **2005**, *24*, 4122.

(4) (a) Braunstein, P.; Boag, N. M. *Angew. Chem., Int. Ed.* **2001**, *40*, 2427. (b) Marks, T. J. *Acc. Chem. Res.* **1992**, *25*, 57.

10.1021/om7007265 CCC: $37.00
Publication on Web 10/31/2007

Chart 1

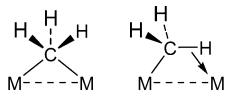

I **II**

classes: those displaying a symmetrical methyl (or alkyl) bridge bound to the dimetal center exclusively through its C atom, then behaving as a one-electron donor (**I** in Chart 1), and those displaying an asymmetrical bridge in which a C−H bond is involved in an α-agostic interaction with one of the metal atoms, the ligand then formally behaving as a three-electron donor (**II** in Chart 1). Among all these metal−metal bonded complexes described so far, however, only a few of them display multiple intermetallic bonding,[6] and their reactivity has not been explored, a circumstance adding further interest to the study of the chemical behavior of the unsaturated methyl complex **2**. In our preliminary report, we proposed for **2** an agostic structure of type **II** on the basis of indirect evidence extracted from ^{31}P NMR data,[1] but this alone constitutes a rather weak support. Besides we must note that the actual coordination mode of the methyl ligand in **2** is relevant to the description of the intermetallic interaction and perhaps also to the reactivity of the molecule: the coordination mode **I** leads to an electron count of 30 (as in the hydride **1**) and therefore to a intermetallic bond of order 3 according to the effective atomic number (EAN) formalism, while the coordination mode **II** yields a 32-electron molecule for which a double intermetallic bond can be proposed. We thus decided to study in detail the structure of this methyl complex both in solution and in the solid state using the pertinent spectroscopic and diffractometric techniques. To get a more complete view of the problem we have also synthesized and fully characterized two closely related compounds: the benzyl complex $[Mo_2Cp_2(\mu\text{-}CH_2Ph)(\mu\text{-}PCy_2)(CO)_2]$ (**3**), in which an α-agostic C−H interaction is also possible, and the phenyl complex $[Mo_2Cp_2(\mu\text{-}Ph)(\mu\text{-}PCy_2)(CO)_2]$ (**4**), for which such an agostic binding cannot take place. We have complemented these experimental studies with density functional theory (DFT) calculations on all three compounds. The bonding in the intermetallic region of the optimized structures has been studied by conventional molecular orbital (MO) analysis and also by inspection of the electron density under the atoms in molecules (AIM) theory.[7] We note that the latter theory has been recently applied to the study of mononuclear complexes displaying agostic C−H−M interactions,[8] but the theoretical analysis of the bonding at binuclear α-agostic complexes of type **II** has been performed previously only in one case and this at the semiempirical level.[9] Finally, to get a more significant interpretation of the results, we have extended our calculations to the hydride-bridged complex **1**. There was an added interest in this last analysis, since previous calculations at different levels on electron-deficient di- or polyhydride complexes having a central $M_2(\mu\text{-}H)_x$ moiety had led to the conclusion that essentially no direct metal−metal bonding results from the tricentric M−H−M interactions there present.[10,11] A similar conclusion was recently reached using DFT calculations on the model molybdenum(III) hydride complex $[Mo_2Cp_2(\mu\text{-}H)(\mu\text{-}PH_2)(\mu\text{-}O_2CH)_2]$.[11] These views, however, are rather inconsistent with the structure and chemical behavior of the molybdenum(II) hydride **1**, and then it was of interest to us a further consideration of the nature of the tricentric $M_2(\mu\text{-}H)$ interaction at our highly unsaturated binuclear substrate.

Results and Discussion

Synthesis of the Hydrocarbyl Complexes 2−4. As stated above, the methyl complex **2** is readily prepared by reacting the anion $[Mo_2Cp_2(\mu\text{-}PCy_2)(\mu\text{-}CO)_2]^-$ (Li^+ salt) with methyl iodide in tetrahydrofuran (THF) solution at room temperature. A similar reaction takes place with benzyl chloride, then giving the benzyl complex **3**. The yields of these products are fair to good (50−65% after purification), but the formation of the corresponding halide derivatives $[Mo_2Cp_2(\mu\text{-}X)(\mu\text{-}PCy_2)(CO)_2]$ (X = Cl, I)[1] as side products in these reactions could not be avoided. The latter seem to arise from a competitive electron-transfer process yet not well understood.

The formation of the phenyl complex **4** requires a different synthetic strategy, since the dimolybdenum anion fails to react with PhX (X = Cl, Br). Actually we found a good preparative route while trying to prepare a molybdenum−lead derivative through the reaction of the dimolybdenum anion with $PbPh_3$-Cl. When carried out in dichloromethane as solvent, this reaction gives compound **4** in high yield, with no intermediates being detected (substantial amounts of $[Mo_2Cp_2(\mu\text{-}Cl)(\mu\text{-}PCy_2)(CO)_2]$ are formed as a side product if tetrahydrofuran is used as solvent). Most likely a triphenyllead intermediate $[Mo_2Cp_2(\mu\text{-}PbPh_3)(\mu\text{-}PCy_2)(CO)_2]$ is first formed, this having a similar structure to that of the unsaturated tin cluster $[Mo_2Cp_2(\mu\text{-}SnPh_3)(\mu\text{-}PCy_2)(CO)_2]$.[2a,b] In a second stage, this lead intermediate would experience phenyl transfer to the dimolybdenum center and elimination of "$PbPh_2$", likely to disproportionate into elemental lead and $PbPh_4$. Indeed, the triphenyllead complex $[WCp(PbPh_3)(CO)_3]$ has been reported to decompose under photochemical treatment to give the phenyl derivative $[WCp(Ph)(CO)_3]$ along with Pb and $PbPh_4$.[12] It is remarkable, however, that the 1,2-phenyl shift responsible for the formation of **4** can occur so rapidly at room temperature, a fact that we attribute to the coordinative and electronic unsaturation of the dimolybdenum center at the Mo_2Pb intermediate first formed.

Solid-State Structures of Compounds 1−4. The structure of compound **1** was confirmed through a single-crystal X-ray diffraction study.[2a] The molecule displays two MoCp(CO) moieties placed in a transoid relative arrangement and bridged

(5) For some recent work on alkyl-bridged complexes see, for example: (a) Bolton P. D.; Clot, E.; Cowley, A. R.; Mountford, P. *J. Am. Chem. Soc.* **2006**, *128*, 15005. (b) Dietrich, H. M.; Grove, H.; Törnroos, K. W.; Anwander, R. *J. Am. Chem. Soc.* **2006**, *128*, 1458. (c) Weng, Z.; Teo, S.; Koh, L. L.; Hor, T. S. A. *Chem. Commun.* **2006**, 1319. (d) Wigginton, J. R.; Trepanier, S. J.; MacDonald, R.; Ferguson, M. J.; Cowie, M. *Organometallics* **2005**, *24*, 6194.

(6) Apparently only a few complexes (all dichromium ones) have been reported to have alkyl bridges across multiple metal−metal bonds: (a) Heintz, R. A.; Ostrander, R. L.; Rheingold, A. L.; Theopold, K. H. *J. Am. Chem. Soc.* **1994**, *116*, 11387. (b) Morse, P. M.; Spencer, M. D.; Wilson, S. R.; Girolami, G. S. *Organometallics* **1994**, *13*, 1646. (c) Andersen, R. A.; Jones, R. A.; Wilkinson, G. *J. Chem. Soc., Dalton Trans.* **1978**, 446.

(7) Bader, R. F. W. *Atoms in Molecules − A Quantum Theory*; Oxford University Press: Oxford, U.K., 1990.

(8) (a) Popelier, P. L. A.; Logothetis, G. *J. Organomet. Chem.* **1998**, *555*, 101. (b) Scherer, W.; Hieringer, W.; Spiegler, M.; Sirsch, P.; McGrady, G. S.; Downs, A. J.; Haaland, A.; Pedersen, B. *Chem. Commun.* **1998**, 2471. (c) Scherer, W.; McGrady, G. S. *Angew. Chem., Int. Ed.* **2004**, *43*, 1782, and references therein. (d) Vidal, I.; Melchor, S.; Alkorta, I.; Elguero, J.; Sundberg, M. R.; Dobado, J. A. *Organometallics* **2006**, *25*, 5638. (e) Brayshaw, S. K.; Green, J. C.; Kociok-Khon, G.; Sceats, E.; Weller, A. S. *Angew. Chem., Int. Ed.* **2006**, *45*, 452.

(9) Bursten, B. E.; Cayton, R. H. *Organometallics* **1986**, *5*, 1051.

(10) (a) Süss-Fink, G.; Therrien, B. *Organometallics* **2007**, *26*, 766. (b) Koga, N.; Morokuma, K. *J. Mol. Struct.* **1993**, *300*, 181. (c) Jezowska-Trzebiatowska, B.; Nissen-Sobocinska, B. *J. Organomet. Chem.* **1988**, *342*, 215.

(11) Baik, M. H.; Friesner, R. A.; Parkin, G. *Polyhedron* **2004**, *23*, 2879.

(12) Pannel, K. H. *J. Organomet. Chem.* **1980**, *198*, 37.

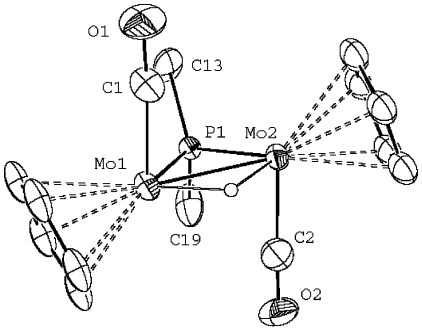

Figure 1. ORTEP diagram of the molecular structure of compound **1** with cyclohexyl rings (except the C^1 atom) and hydrogen atoms (except the hydride atom) omitted for clarity. Reproduced with permission from ref 2a. Copyright 2005 American Chemical Society.

Table 1. Selected Bond Lengths and Angles for Compounds 1−4

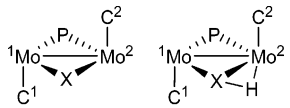

param[a]	**1**[b]	**2**[c]	**3**	**4**
Mo1−Mo2	2.528(2)	2.558(2)	2.580(1)	2.557(2)
Mo1−P	2.382(3)	2.384(1)	2.395(2)	2.396(3)
Mo1−C1	1.92(1)	1.923(3)	1.935(7)	1.94(1)
Mo1−X	1.88(10)	2.28(1)	2.294(7)	2.31(1)
Mo2−P	2.386(3)	2.382(2)	2.406(2)	2.386(3)
Mo2−C2	1.90(1)	1.925(3)	1.917(7)	1.94(1)
Mo2−X	1.84(8)	2.43(1)	2.416(7)	2.39(1)
C1−Mo1−Mo2	79.7(4)	78.5(1)	84.3(2)	79.2(5)
C2−Mo2−Mo1	80.1(2)	78.6(1)	73.8(2)	83.6(4)
Mo1−P−Mo2	64.0(1)	64.9(1)	65.0(1)	64.6(1)
Mo1−X−Mo2	85(4)	65.8(3)	66.4(2)	65.9(3)
Mo2−H		2.27(5)	2.06(5)[d]	

[a] Values in angstroms or degrees, respectively, according to the labeling shown in the figures; X = H (**1**) or C (**2**−**4**). [b] Data taken from ref 2a. [c] Data involving the disordered methyl group correspond to those of site A in the crystal (50% occupancy, see text). [d] X−H, 1.03(6); X−H (nonagostic), 1.01(7); X−C(Ph), 1.521(9) Å.

by hydride and dicyclohexylphosphide ligands (Figure 1 and Table 1). The carbonyl ligands are almost perpendicular to the intermetallic vector (slightly bent over it, with Mo−Mo−C angles of ca. 80°) so that the overall geometry of the complex can be described approximately as edge-bridging bioctahedral, if we take the cyclopentadienyl ligand as equivalent to three facial terminal groups. According to the EAN formalism, a triple Mo−Mo bond must be formulated for this 30-electron complex, which is in agreement with the very short intermetallic length, 2.528(2) Å, ca. 0.7 Å shorter than the corresponding distance in the 34-electron hydrides $[Mo_2Cp_2(\mu\text{-H})(\mu\text{-PRR}')(CO)_4]$ (ca. 3.25−3.28 Å),[13] and similar to the values found for related cyclopentadienyl complexes having triple intermetallic bonds bridged by dialkyl- or diarylphosphide ligands, such as $[Mo_2Cp_2(\mu\text{-COEt})(\mu\text{-PCy}_2)(\mu\text{-CO})]$ (2.478(1) Å),[1] $[Mo_2Cp_2(\mu\text{-PPh}_2)_2(\mu\text{-CO})]$ (2.515(2) Å),[14a] and $[Mo_2Cp_2(\mu\text{-PhPC}_6H_4PPh)(\mu\text{-CO})]$ (2.532(1) Å),[14b] or the phosphinidene complex $[Mo_2Cp_2(\mu\text{-PR*})(\mu\text{-CO})_2]$ (2.5322(3) Å; R* = 2,3,5-$C_6H_2{}^t\text{Bu}_3$).[15] The structures of compounds **2**−**4** (Figures 2−4) are very similar to that of **1**, after replacing the bridging hydrogen atom by methyl (**2**), benzyl (**3**), or phenyl (**4**) ligands, but the coordination of these groups is not identical.

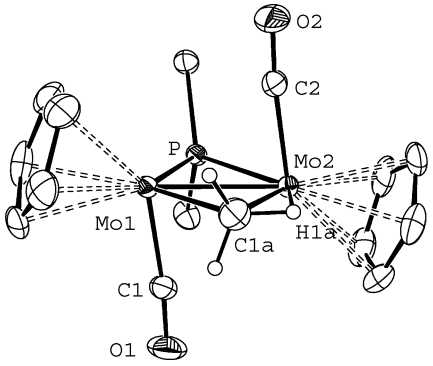

Figure 2. ORTEP diagram (30% probability) of the molecular structure of compound **2**, with cyclohexyl rings (except the C^1 atom) and hydrogen atoms (except those of the methyl group) omitted for clarity. Only one of the two sites of the methyl ligand are shown (50% occupancy, see text).

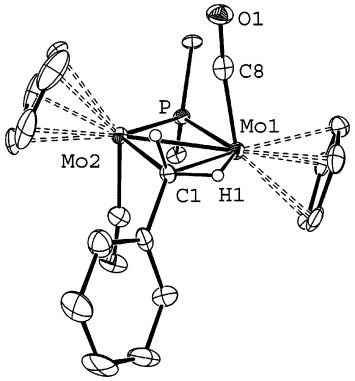

Figure 3. ORTEP diagram (30% probability) of the molecular structure of compound **3**, with cyclohexyl rings (except the C^1 atom) and hydrogen atoms (except those of the benzyl group) omitted for clarity.

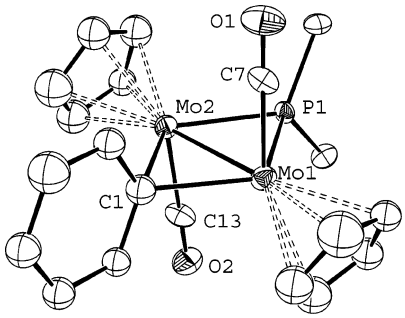

Figure 4. ORTEP diagram (25% probability) of the molecular structure of compound **4**, with cyclohexyl rings (except the C^1 atom) and hydrogen atoms omitted for clarity.

In the crystals of **2**, the methyl group is disordered and it was successfully refined as an asymmetric bridge of type II placed at two close sites with half-occupancy (only one of them shown in Figure 2). In spite of the agostic C(1)−H(1)···Mo(2) interaction there involved, the intermetallic distance of 2.558(2) Å is only 0.03 Å longer than that in **1**, this suggesting that

(13) (a) Alvarez, C. M.; Alvarez, M. A.; García-Vivó, D.; García, M. E.; Ruiz, M. A.; Sáez, D.; Falvello, L. R.; Soler, T.; Herson, P. *Dalton. Trans.* **2004**, 4168. (b) Alvarez, C. M.; Alvarez, M. A.; Alonso, M.; García, M. E.; Ruiz, M. A. *Inorg. Chem.* **2006**, *45*, 9593.

(14) (a) Adatia, T.; McPartlin, M.; Mays, M. J.; Morris, M. J.; Raithby, P. R. *J. Chem. Soc., Dalton Trans.* **1989**, 1555. (b) Kyba, E. P.; Mather, J. D.; Hasset, K. L.; McKennis, J. S.; Davis, R. E. *J. Am. Chem. Soc.* **1984**, *106*, 5371.

(15) Amor, I.; García, M. E.; Ruiz, M. A.; Sáez, D.; Hamidov, H.; Jeffery, J. C. *Organometallics* **2006**, *25*, 4857.

such an interaction is rather weak. Interestingly, the average Mo−C(1) distances of ca. 2.35 Å are only slightly longer than "normal" single bond Mo−CH_3 lengths (for example, ca. 2.30 Å for methyl complexes of type [MoL(CO)$_3$Me], with L = substituted η^5-Cp ligand),[16] which suggests that the three-center−two-electron (3c−2e) interaction between the carbon atom and the molybdenum atoms is quite strong, perhaps as a result of the coordinative and electronic unsaturation of the dimetal center. There is only one other methyl-bridged dimolybdenum complex structurally characterized previously, [Mo_2Cp*$_2$(μ-Me)(μ-PMe$_2$)(μ-O_2CMe)$_2$],[17] which however exhibits a symmetrically bridged methyl group of type I. The Mo−C lengths in the latter (ca. 2.30 Å) are even shorter than those in **2**, perhaps due to the higher oxidation state (III) of the Mo atoms in that acetate complex and the absence of agostic interactions.

The benzyl ligand in **3** also exhibits an asymmetrical coordination of type II, being bound to one of the metal atoms through a "normal" single bond (Mo−C =2.294(7) Å) and involved in an agostic interaction with the second metal atom, with Mo−C and Mo−H lengths of 2.417(6) and 2.06(5) Å, respectively (note that the latter distance approaches the Mo−H(hydride) lengths in compound **1**). The geometric asymmetry [Δd(Mo−C)] of the bridgehead carbon atom is thus of 0.123 Å, which can be considered as moderate when compared to those found in other α-agostic alkyl complexes such as [Mo_2Cp$_2$(μ-SMe)$_3${μ-CH_2CH_2(*p*-tol)}]BF$_4$ (Δd = 0.16 Å),[18] [Fe_2Cp$_2$(μ-Me)(μ-CO)(μ-dppm)]PF$_6$ (Δd = 0.10 Å),[19] [ReW{μ-CH_2(*p*-tol)}(μ-CO)(CO)$_6$(μ-dppm)] (Δd = 0.24 Å),[20] or [Mn_2(μ-CH_2R)$_2$(CH_2R)$_2$(PR′$_2$R″)$_2$] (R = Ph, $SiMe_3$, ^{t}Bu; Δd = 0.16−0.20 Å).[21] This suggests that the agostic interaction of the benzyl ligand in complex **3** is also rather weak, in agreement with the spectroscopic data and theoretical calculations to be discussed later on. In any case, the asymmetry of the benzyl coordination seems to be geometrically compensated by the significant dissymmetry of the carbonyl ligands, with one of them opening away from and the other bending over the intermetallic vector (C−Mo−Mo angles, ca. ±5° relative to the angles in the "symmetrical" complex **1**; in a formal sense, the agostic coordination of the benzyl group makes this ligand act as a donor of more than one electron (three, in its extreme view), this rendering a less unsaturated dimetal center, so the intermetallic interaction should be weakened accordingly. Indeed, the intermetallic distance in **3** is somewhat longer than that in **2** (by ca. 0.02 Å) or **1** (by ca. 0.05 Å), but still is substantially shorter than the reference values of ca. 2.65−2.70 Å found for comparable 32-electron complexes (cf. 2.716(1) Å in [Mo_2Cp$_2$(μ-PPh$_2$)$_2$(CO)$_2$][14a] or 2.6550(5) Å in [Mo_2Cp$_2$(μ-PCy$_2$){η^2:η^2-C_2(OMe)$_2$}(CN^tBu)$_2$]BF$_4$).[3] This again suggests that the agostic interaction present in **3** is one of a rather low strength.

As for the structure of the phenyl complex **4**, first we must say that all our attempts to crystallize it led to twinned crystals. The bad quality of the diffraction data thus precluded the anisotropic refinement of the C atoms, and therefore a detailed analysis of the Mo−C or C−C lengths, but still yielded a reasonable picture of the structure of the complex. The molecule displays a phenyl ring bridging the dimetal center through its ipso-C atom, with the ring being almost perpendicular to the intermetallic vector. The bonded carbon atom is placed asymmetrically, being closer to the Mo(1) center (Δd = 0.08 Å), which seems to be compensated by a slightly closer approach of the P atom to Mo(2) and a distinct degree of bending of the carbonyls toward the intermetallic vector (C−Mo−Mo angles, ca. 80 and 84°), as observed in the agostic benzyl complex. This asymmetry in the phenyl coordination does not appear to have an intramolecular origin and is probably due to packing forces in the crystal. Indeed, the DFT-optimized structure for this complex shows an equidistant positioning of the phenyl ring over the Mo−Mo vector, as it will be discussed later on. In any case, this η^1-coordination of the phenyl ligand in principle makes it a one-electron donor, so that compound **4** should be considered isoelectronic with the hydride complex **1**. In agreement with this, the intermetallic length in **4** is only 0.03 Å longer than that in **1**. However, although no other phenyl-bridged dimolybdenum complex appears to have been structurally characterized, and therefore direct comparisons are not possible, we trust that the average Mo−C(Ph) length of 2.35 Å in **4** must be considered as rather short for a tricentric interaction, since this value is similar to that measured for the "regular" (bicentric) Mo−C(phenyl) bond in the Mo(II) complex [MoCp(Ph)(CO)$_2$(PPh$_3$)] (2.334(2) Å).[22] Finally, we must note that although a considerable number of phenyl-bridged di- and polynuclear transition-metal complexes are currently known, most of these species display just single metal−metal bonds. In fact, to our knowledge there is only one other clear example in which a phenyl ligand bridges a multiple intermetallic bond, this being the recently reported 32-electron diruthenium cation [Ru_2Cp*$_2$(μ-Ph)(μ-H)(μ-PPh$_2$)]$^+$.[23] We note also that a related family of unsaturated alkyl- and phenyl-bridged dichromium species of general formula [Cr_2Cp*$_2$(μ-R)(μ-R′)] (R, R′ = alkyl, Ph) has been reported previously, although the nature of the intermetallic interaction in these complexes is not clear.[6a] We must remark here that the presence of a multiple metal−metal bond is a significant feature in the structure of binuclear alkyl- or aryl-bridged binuclear complex because its presence may induce or allow the occurrence of additional interactions between the bridging ligands and the dimetal center, a matter also to be discussed later on.

Table 2. Selected IR[a] and ^{31}P{^{1}H} NMR[b] Data for Compounds 1−4

compd	ν(CO)	δ_P
[Mo_2Cp$_2$(μ-H)(μ-PCy$_2$)(CO)$_2$] (**1**)	1858 (m),[c] 1829 (vs)	232.3
[Mo_2Cp$_2$(μ-CH_3)(μ-PCy$_2$)(CO)$_2$] (**2**)	1854 (m),[c] 1815 (vs)	153.3
[Mo_2Cp$_2$(μ-CH_2Ph)(μ-PCy$_2$)(CO)$_2$] (**3**)	1860 (m),[c] 1825 (vs)	147.7 [d]
[Mo_2Cp$_2$(μ-Ph)(μ-PCy$_2$)(CO)$_2$] (**4**)	1849 (m),[c] 1812 (vs)	174.8 [e]

[a] Recorded in dichloromethane solution, unless otherwise stated; ν in cm^{-1}. [b] Recorded in CD_2Cl_2 solutions at 290 K and 121.50 MHz, unless otherwise stated; δ in ppm relative to external 85% aqueous H_3PO_4. [c] Shoulder. [d] Recorded at 81.02 MHz. [e] Recorded in $CDCl_3$.

Solution Structure of the Hydride Complex 1. The spectroscopic data in solution for compound **1** (Table 2 and Experimental Section) are in general agreement with the

(16) (a) Zhao, J.; Santos, A. M.; Herdtweck, E.; Kühn, F. E. *J. Mol. Catal. A: Chem.* **2004**, *222*, 265. (b) Körnich, J.; Haubold, S.; He, J.; Reimelt, O.; Heck, J. *J. Organomet. Chem.* **1999**, *584*, 329. (c) El Mouatassim, B.; Elamouri, H.; Vaissermann, J.; Jaouen, G. *Organometallics* **1995**, *14*, 3296. (d) Rogers, R. D.; Atwood, J. L.; Rausch, M. D.; Macomber, D. W. *J. Chem. Crystallogr.* **1990**, *20*, 555.

(17) Parkin, G.; Shin, J. H. *Chem. Commun.* **1998**, 1273.

(18) Cabon, N.; Le Goff, A.; Le Roy, C.; Pétillon, F. Y.; Schollhammer, P.; Talarmin, J.; McGrady, J. E.; Muir, K. W. *Organometallics* **2005**, *24*, 6268.

(19) Dawkins, G. M.; Green, M.; Orpen, A. G.; Stone, F. G. A. *J. Chem. Soc., Chem. Commun.* **1982**, 41.

(20) Jeffery, J. C.; Orpen, A. G.; Stone, F. G. A.; Went, M. J. *J. Chem. Soc., Dalton Trans.* **1986**, 173.

(21) Howard, C. G.; Wilkinson, G.; Thornton-Pett, M.; Hursthouse, M. B. *J. Chem. Soc., Dalton Trans.* **1983**, 2025.

(22) Butters, T.; Winter, W.; Kunze, U.; Sastrawan, S. B. *Acta Crystallogr., Sect. C: Cryst. Struct. Commun.* **1985**, *41*, 23.

(23) Tschan, M. J. L.; Chérioux, F.; Karmazin-Brelot, L.; Süss-Fink, G. *Organometallics* **2005**, *24*, 1974.

structure found in the crystal, but they also reveal the occurrence of some dynamic processes in solution. The IR spectrum of **1** exhibits two C−O stretching bands with the relative intensities (weak and strong, in order of decreasing frequency) characteristic of transoid $M_2(CO)_2$ oscillators[24] and frequencies a bit lower than those measured for the bis(phosphide) complexes of the type *trans*-$[Mo_2Cp_2(\mu\text{-}PR_2)(\mu\text{-}PR_{2'})(CO)_2]$,[25] as expected. The chemical shift of the ^{31}P nucleus in **1** (232.3 ppm), however, is much higher than the values of ca. 100 ppm observed for the PCy_2 bridges in the above 32-electron compounds, and in fact is very similar to those measured for the 30-electron monocarbonyls $[Mo_2Cp_2(\mu\text{-}PR_2)(\mu\text{-}PR_{2'})(\mu\text{-}CO)]$ (ca. 240−260 ppm for PCy_2 bridges).[25] Although there are many factors affecting the ^{31}P chemical shifts of dialkyl- and diarylphosphide bridging ligands (C−P−C and M−P−M angles, M−M and M−P lengths, etc),[26,27] it is clear that a relationship exists between the ^{31}P chemical shifts of the PCy_2 groups and the electron-donor properties of the bridging X groups (and hence the total electron count of the molecule) in dicarbonyl complexes of the type *trans*-$[Mo_2Cp_2(\mu\text{-}PCy_2)(\mu\text{-}X)(CO)_2]$. Actually we can conclude that, within this structural family, the 32-electron complexes having three-electron donor X bridges tend to display ^{31}P shifts some 100 ppm lower than do 30-electron molecules having one-electron X bridges, as illustrated by the following sequence of X(δ_P/ppm): $SnPh_3(248.5)$[2a,b] > H(232.3) > $AuPPh_3(213.9)$[1] > Cl(155.6)[1] > $\eta^1{:}\eta^2$-CMe═CH_2(131.2)[1] > C−CO_2Me(128.2)[3] > N═CHPh(125.4)[2d] > $P(OEt)_2(119.5)$[1] > $PCy_2(95.4)$.[25] This relationship will be of relevance when analyzing the solution structure of the alkyl derivatives **2** and **3** or that of the phenyl complex **4**.

The ^1H NMR spectrum of **1** exhibits a single resonance for the equivalent cyclopentadienyl ligands as expected, but the hydride resonance (δ_H, −6.94 ppm; J_{PH} = 11 Hz) appears at a frequency higher, and with lower P−H coupling, than those of the related 34-electron complexes $[Mo_2Cp_2(\mu\text{-}H)(\mu\text{-}PRR')(CO)_4]$ (ca. δ_H, −11 to −13 ppm; J_{PH} = 35−40 Hz).[13,25] The lower value of the P−H coupling in **1** can be explained from the known trends for $^2J_{XY}$ in complexes of the type $[MCpXYL_2]$,[28,29] since the H−Mo−P angle in **1** (ca. 105°) is much higher than the values of ca. 75° in the 34-electron hydrides. The relatively low shielding of the hydride nucleus, however, is anomalous and must be related to the strong magnetic anisotropy of the multiple metal−metal bonds.[30] Indeed we have previously reported very low shieldings for the hydride bridges in the 30-electron complexes $[W_2Cp_2(\mu\text{-}H)(CO)_2L_2]^+$ (δ_H, ca. −2.5 ppm; L_2 = $R_2PCH_2PR_2$; R = Ph, Me)[31] and $[Mo_2Cp_2(\mu\text{-}H)(SnPh_3)(CO)_2(PHCy_2)]$ (δ_H, −1.98 ppm).[2b] Note that all these complexes have a single hydrogen atom bridging over a (formal) triple bond, as it is the case of **1**. In contrast, 30-electron complexes having a number of hydride bridges equal to or higher than 3 (the formal bond order according to the EAN formalism) display the usual strongly shielded resonances of bridging hydrides, as it is the case of the complexes $[M_2Cp_2(\mu\text{-}H)_4]$ (M= Fe, Ru)[32] and $[Ru_2(\eta^6\text{-}C_6Me_6)_2(\mu\text{-}H)_3]^+$.[10a] As stated above, in the latter complexes there is little direct intermetallic interaction, which is mostly made up of tricentric M−H−M interactions (which are in fact the same type of interactions present in electron-precise complexes). As it will be seen later on, however, the intermetallic interaction in **1** is made up of a tricentric Mo−H−Mo bond and two direct (σ and π) Mo−Mo interactions, and it must be the magnetic anisotropy of that electron distribution that causes the relative deshielding of the hydride nucleus. It is tempting to use the known anisotropic properties of double C−C bonds[33] as a qualitative model for π_{MM} bonds, this leading to the prediction that the hydride ligand in **1** might experience a significant deshielding influence from the π_{MoMo} electrons, since this H nucleus is placed in the nodal plane of that bond (see below).

Scheme 1. Carbonyl Exchange Process Proposed for Compound 1 in Solution (Substituents on Phosphorus Omitted for Clarity)

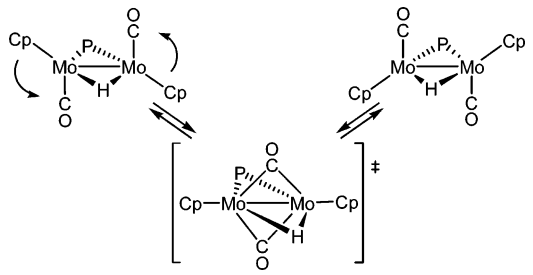

The variable-temperature $^{13}C\{^1H\}$ NMR spectra of **1** indicate dynamic behavior in solution (see Experimental Section). When recorded in dichloromethane solutions at 253 K, the spectrum is fully consistent with the solid-state structure, which implies the presence of a C_2 axis relating the pairs of Cp, CO, and Cy groups. On lowering the temperature, however, the chemical equivalence of the two Cy groups seems to disappear, since the resonances for the C^1 and one of the C^2 nuclei broaden severely below 213 K, almost disappearing in the baseline at the lowest temperature analyzed (188 K), while the rest of the resonances remain essentially unchanged. We interpret this as possibly resulting from an arrested rotation around the P−C(Cy) bonds at those temperatures. More interesting, however, is the fact that dynamic effects are present also above 253 K. Thus, upon increasing the temperature, the resonances of the diastereotopic pairs of C^2 and C^3 atoms of the cyclohexyl rings first broaden and then eventually coalesce into a single resonance in each case. From the corresponding coalescence temperatures (ca. 318 K for the C^3 resonances and 338 K for the C^2 resonances, when recorded at 100.63 MHz in toluene-d_8 solution) we can estimate a single activation barrier of 68 ± 1 kJ mol^{-1} for the undergoing process.[34] For this we propose a concerted exchange of the carbonyl ligands (Scheme 1), similar to that involving the linear semibridging carbonyls in the

(24) Braterman, P. S. *Metal Carbonyl Spectra*; Academic Press: London, U.K., 1975.

(25) García, M. E.; Riera, V.; Ruiz, M. A; Rueda, M. T.; Sáez. D. *Organometallics* **2002**, *21*, 5515.

(26) Carty, A. J.; MacLaughlin, S. A.; Nucciarone, D. In *Phosphorus-31 NMR Spectroscopy in Stereochemical Analysis*; Verkade, J. G., Quin, L. D., Eds.; VCH: Deerfield Beach, FL, 1987; Chapter 16.

(27) (a) Carty, A. J.; Fyfe, C. A.; Lettinga, M.; Johnson, S.; Randall, L. H. *Inorg. Chem.* **1989**, *28*, 4120. (b) Eichele, K.; Wasylishen, R. E.; Corrigan, J. F.; Taylor, N. J.; Carty, A. J.; Feindel, K. W.; Bernard, G. M. *J. Am. Chem. Soc*. **2002**, *124*, 1541.

(28) Jameson, C. J. In *Phosphorus-31 NMR Spectroscopy in Stereochemical Analysis*; Verkade, J. G., Quin, L. D., Eds.; VCH: Deerfield Beach, FL, 1987; Chapter 6.

(29) Wrackmeyer, B.; Alt, H. G.; Maisel, H. E. *J. Organomet. Chem.* **1990**, *399*, 125.

(30) Cotton, F. A. In *Multiple Bonds between Metal Atoms*, 3rd ed.; Cotton, F. A., Murillo, C. A., Walton, R. A., Eds.; Springer: New York, 2005; Chapter 16, p 720.

(31) Alvarez, M. A.; García, M. E.; Riera, V.; Ruiz, M. A. *Organometallics* **1999**, *18*, 634.

(32) Suzuki, H. *Eur. J. Inorg. Chem.* **2002**, 1009, and references therein.

(33) Günther, H. *NMR Spectroscopy*; Wiley: Chichester, U.K., 1980; p 70.

(34) Calculated using the modified Eyring equation $\Delta G^{\ddagger} = 19.14T_c[9.97 + \log(T_c/\Delta\nu)]$ (J mol^{-1}). See ref 33, p 243.

Scheme 2. Overall Fluxional Process Proposed for Compound 3 in Solution (Substituents on Phosphorus Omitted for Clarity)

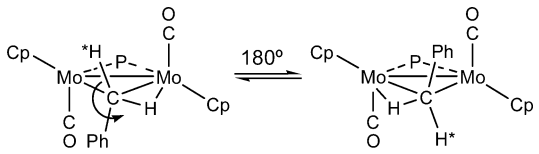

isoelectronic complexes $[MoWCp_2(CO)_4]$[35a] and $[Mo_2Cp_2(CO)_3L]$ ($L = P(Ph)(OCH_2CH_2)_2NH$).[35b] In the latter complexes, the scrambling process has a low barrier of ca. 45 kJ mol^{-1}. In the case of **1**, however, the CO ligands are almost terminally bound, and then a greater reorganization is needed to reach the carbonyl-bridged transition state, thus explaining the considerably higher value of the activation barrier in our case.

Solution Structure of the Alkyl Complexes 2 and 3. The spectroscopic data for complex **3** indicate that the agostic coordination mode for the benzyl bridge found in the crystal is essentially retained in solution. Thus, the ^{31}P spectrum displays a resonance at 147.7 ppm, in the region of the 32-electron complexes mentioned above (cf. 131.2 ppm for $[Mo_2Cp_2(\mu\text{-}\eta^1\text{:}\eta^2\text{-}CMe{=}CH_2)(\mu\text{-}PCy_2)(CO)_2]$),[1] thus suggesting a three-electron-like contribution of the benzyl ligand. The ^{1}H NMR data confirm this view, although revealing again the occurrence of dynamic processes (see Experimental Section). At room temperature the methylenic protons of the benzyl group give rise to two distinct NMR resonances at 2.46 and −1.35 ppm. The significant shielding of the latter is indicative of the presence of an agostic C−H···M interaction, as it is the observation of a reduced coupling of 100 Hz for the corresponding ^{13}C NMR resonance (δ_C −4.2 ppm; J_{CH} = 130 and 100 Hz), in the upper extreme of the usual range of 75−100 Hz.[36] Moreover, these values are comparable to those observed previously for binuclear complexes having α-agostic CH_2R bridges over electron-precise Mo_2 or RhOs centers.[18,37] In the WRe complex $[ReW\{\mu\text{-}CH_2(p\text{-tol})\}(\mu\text{-}CO)(CO)_6(\mu\text{-}Ph_2PCH_2PPh_2)]$, however, a more reduced C−H coupling of 81 Hz was measured.[20] All the above data point to the presence of a rather weak agostic interaction in solution for compound **3**.

As stated above, the NMR spectra of **3** also reveal the presence of dynamic processes in solution. In the first place, the room-temperature ^{1}H and $^{13}C\{^1H\}$ NMR spectra are not fully consistent with the static structure, since they exhibit single resonances for the inequivalent CO and Cp ligands, as well as a single set of six resonances for the inequivalent cyclohexyl rings. On lowering the temperature, two significant spectroscopic changes occur in the ^{1}H NMR spectra. First, the cyclopentadienyl resonance at 5.17 ppm broadens and eventually splits into two well-separated singlets at 5.46 and 5.04 ppm. From the coalescence temperature (218 K, when measured in CD_2Cl_2 at 400.13 MHz) we can estimate a barrier of 42 ± 1 kJ mol^{-1} for the corresponding process.[34] For this we propose a 180° rotation of the benzyl group around the C···P vector (Scheme 2), which effectively creates a false C_2 axis relating both metal centers, then explaining the apparent equivalence of the pairs of carbonyl, cyclopentadienyl, and cyclohexyl groups. This process does not create a mirror plane relating the metal centers, and therefore the diastereotopic pairs of carbon atoms of the Cy rings (C^2 and C^3) must remain inequivalent, as observed. It is interesting to note that similar energy barriers have been calculated for the opening of the two α-agostic interactions present in the quadruply bonded dichromium anion $[Cr_2(\mu\text{-}CH_2SiMe_3)_2(CH_2SiMe_3)_4]^{2-}$ (40 kJ mol^{-1})[6b] or for the exchange between agostic and nonagostic protons in the methyl-bridged complex $[Cp_2Ti(\mu\text{-}Me)(\mu\text{-}CH_2)Rh(COD)]$ (41 kJ mol^{-1}).[38] In contrast, the barrier estimated for the proton exchange within the methyl bridge in the cluster $[Os_3(\mu\text{-}H)(\mu\text{-}CH_3)(CO)_{10}]$ is only of ca. 15 kJ mol^{-1}.[39] The distinct steric crowding around the alkyl bridges may be more relevant at defining their dynamic behavior than the intrinsic strength of the agostic interactions in all these complexes. Interestingly, in the model dimolybdenum complex $[Mo_2Cp_2(\mu\text{-}SH)_3(\mu\text{-}CH_2CH_2Ph)]BF_4$ it has been calculated using DFT methods that the rotation of the α-agostic CH_2CH_2Ph group (so as to exchange the agostic and nonagostic hydrogens) has a barrier of 46 or just 13 kJ mol^{-1} depending on whether the CH_2CH_2Ph residue crosses or not the Mo_2C plane during the rotation, the difference being mainly due to the much greater steric repulsions with the Cp rings in the first case.[18] In the case of **3**, such a proton exchange would in fact be an isomerization, which is not observed, perhaps due to even more severe repulsions between the Ph residue and the closer Cp ligand. However, the proposed 180° rotation yet implies the crossing of the Ph residue from one to the other side of the Mo_2C plane, thus accounting for the relatively high barrier found.

The second spectroscopic change observed for **3** on lowering the temperature is the progressive shift of the methylenic resonances away from each other, so the average shifts are ca. −0.0039 (nonagostic) and +0.0056 ppm/K (agostic) in the range of 193−293 K. The same is observed when heating toluene-d_8 solutions of **3** up to 378 K, the resonances now approaching each other at similar average rates of −0.0041 (nonagostic) and +0.0068 ppm/K (agostic), without experiencing significant broadening. These shifts are not related to the fluxional process just discussed (would such a process imply the exchange between the methylenic protons, then the width line of these resonances would be higher than 500 Hz at 378 K!). Interestingly, we note that the complex $[ReW\{\mu\text{-}CH_2(p\text{-tol})\}(\mu\text{-}CO)(CO)_6(\mu\text{-}Ph_2PCH_2PPh_2)]$ was reported to experience an overall shielding of 0.40 ppm from 293 to 193 K (similar to that observed for **3**) for the agostic resonance, although the equilibrium between the isomers implied could not be identified at the time.[20] In the case of **3**, we propose that in solution the agostic structure of type II (**3-II**) coexists with a very small amount of a nonagostic structure of type I (**3-I**), they being in fast equilibrium on the NMR time scale at all temperatures studied. In fact, structures of type I (several rotamers are possible) must be intermediates in the fluxional process experienced by the major agostic isomer, since they are related by the progressive rotation of the benzyl group (Scheme 3). Very likely, the ^{1}H NMR resonances for the diastereotopic methylenic protons in **3-I** would have shifts intermediate between those of the agostic isomer. Thus, the mutual approach of the methylenic resonances observed for **3** on raising the temperature would result from a slight increase in the equilibrium amount of the nonagostic isomer **3-I** at high temperatures.

(35) (a) Curtis, M. D.; Fotinos, N. A.; Messerle, L.; Sattelberger, A. *Inorg. Chem.* **1983**, *22*, 1559. (b) Wachter, J.; Riess, J. G.; Mitschler, A. *Organometallics* **1984**, *3*, 714.

(36) Brookhart, M.; Green, M. L. H. *J. Organomet. Chem.* **1983**, *250*, 395.

(37) (a) Wigginton, J. R.; Chokshi, A.; Graham, T. W.; McDonald, R.; Ferguson, M. J.; Cowie, M. *Organometallics* **2005**, *24*, 6398. (b) Trepanier, S. J.; Dennett, J. N. L.; Sterenberg, B. T.; McDonald, M. J.; Cowie, M. *J. Am. Chem. Soc.* **2004**, *126*, 8046.

(38) Ozawa, F.; Park, J. W.; Mackenzie, P. B.; Schaefer, W. P.; Henling, L. M.; Grubbs, R. H. *J. Am. Chem. Soc.* **1989**, *111*, 1319.

(39) Koike, M.; VanderVelde, D. G.; Shapley, J. R. *Organometallics* **1994**, *13*, 1404.

Scheme 3. Fluxionality and Isomerization Processes Proposed for Compound 3 in Solution (Substituents on Phosphorus Omitted for Clarity)

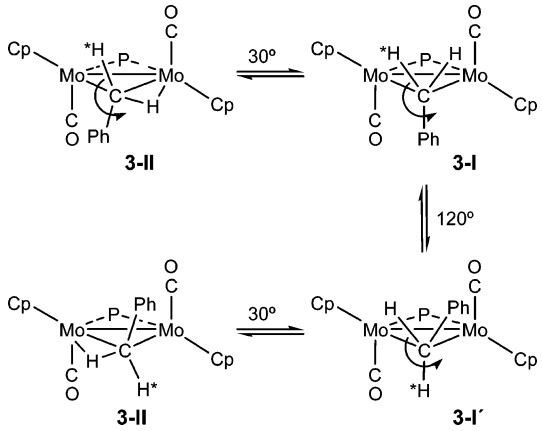

Scheme 4. Dynamic Process Proposed for Compound 2 in Solution (Substituents on Phosphorus Omitted for Clarity; Only the First Steps Shown)

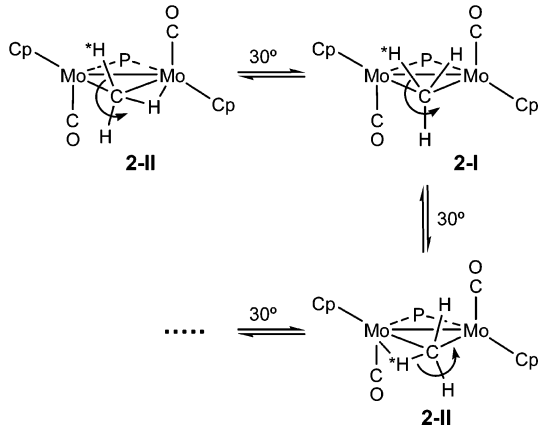

To find supporting evidence for the above hypothesis, the **3-I** structure was optimized imposing geometric constraints on the torsion of the methylenic protons. Subsequent frequency calculation for this structure gives an imaginary frequency that corresponds to the torsion of the CH_2Ph group with respect to the Mo−Mo segment. This is an agreement with the fact that the true minimum of **3** is associated with the **3-II** structure. The differences in the thermodynamic functions at 298.15 K between the structures **3-II** and **3-I** are as follows: $\Delta G_{298} = -34.4$ kJ mol^{-1}, $\Delta H_{298} = -28.4$ kJ mol^{-1}, and $\Delta S_{298} = 20.2$ J mol^{-1} K^{-1}. These values support the hypothesis that, in solution, a certain amount of the **3-I** isomer might be present in equilibrium with the dominant **3-II** form.

Spectroscopic data for the methyl complex **2** suggest that an agostic structure of type II is also dominant in solution. Thus, its ^{31}P chemical shift (153.3 ppm) is very similar to that of **3**, which suggests a three-electron-like contribution of the methyl group to the metal center. In the same line, the DFT optimized structure for this complex also yields an agostic methyl bridge, as it will be discussed later on. However, direct spectroscopic evidence for the presence of an agostic C−H···Mo interaction in solution for **2** could not be found. In fact, the ^{1}H NMR spectra of **2** exhibit a single resonance at ca. −0.7 ppm for the three H atoms of the methyl group in the range of 183−378 K and display no noticeable temperature dependence. In addition, the Cp ligands remain equivalent in the same range. At the same time, the methyl ^{13}C NMR resonance appears at ca. −44 ppm and exhibits only a marginally reduced C−H coupling of 124 Hz. All this suggests the operation of a fast fluxional process in solution now exchanging the chemical environments of the three methyl protons. For this we propose a stepwise rotation of the methyl group around the C···P vector, similar to that proposed for the benzyl group of **3** and perhaps also implying the presence of small amounts of the nonagostic structure **2-I**, but now made up of only 30° rotation steps, then implying the exchange between agostic and nonagostic positions and also rendering in the end an apparent C_2 symmetry axis (Scheme 4). Taking the value of 130 Hz as a reference coupling for a regular C−H bond, then the average value of 124 Hz suggests a figure of ca. 112 Hz for the C−H coupling in the agostic bond of **2**, which points to a weaker agostic interaction when compared to that in **3** ($J_{CH} = 100$ Hz), in agreement with theoretical calculations to be discussed later on. In any case, we note that the above spectroscopic parameters are similar to those previously reported for complexes having agostic methyl bridges of type II over Os_2,[40] Fe_2,[19,41] Ru_2,[42] Re_2,[43] and heterometallic TiM (M = Rh, Pt)[38,44] or RhM centers (M = Ru, Os),[5d,45] all of which are also highly fluxional in solution. In the dimolybdenum complex $[Mo_2Cp^*_2(\mu\text{-Me})(\mu\text{-PMe}_2)(\mu\text{-O}_2\text{CMe})_2]$[17] (structure of type I in the solid state), a C−H coupling of 113 Hz was measured for the methyl bridge, but this low value was attributed by the authors to a diminished *s*-orbital contribution to the C−H bond;[17] apparently, the possibility of having in solution an agostic structure of type II was discarded at the time.

Solution Structure of the Phenyl Complex 4. The spectroscopic data in solution for this molecule do not reveal the presence of dynamic processes and are fully consistent with the structure found in the solid state, which imply the chemical equivalence of the pairs of Cp, CO, and Cy groups, as well as the equivalence of the pairs of C^2 and C^3 atoms of the phenyl ring (but not those of the Cy groups, which remain diastereotopic). The ^{1}H NMR resonances of the phenyl ligand in **4** are not remarkable when compared to those previously reported for other complexes having symmetrical phenyl bridges,[23,46] but the ^{13}C NMR resonances for the ipso- and ortho-carbon atoms are rather unusual. The former gives rise to a quite shielded resonance at 125.8 ppm, whereas this resonance is usually the most deshielded one of a phenyl ligand not only in terminal,[47] but even in bridging complexes,[46] although the amount of ^{13}C NMR data available here is rather limited in general, and inexistent in the case of the group 6 metal complexes. At the

(40) (a) Calvert, R. B.; Shapley, J. R. *J. Am. Chem. Soc.* **1977**, *99*, 5225. (b) Calvert, R. B.; Shapley, J. R. *J. Am. Chem. Soc.* **1978**, *100*, 7726.

(41) Casey, C. P.; Fagan, P. J.; Miles, W. H. *J. Am. Chem. Soc.* **1982**, *104*, 1134.

(42) (a) Davies, D. L.; Gracey, B. P.; Guerchais, V.; Knox, S. A. R.; Orpen, A. G. *J. Chem. Soc., Chem. Commun.* **1984**, 841. (b) Gao, Y.; Jennings, M. C.; Puddephatt, R. J. *Organometallics* **2001**, *20*, 1882.

(43) Carlucci, L.; Proserpio, D. M.; D'Alfonso, G. *Organometallics* **1999**, *18*, 2091.

(44) Park, J. W.; Mackenzie, P. B.; Schaefer, W. P.; Grubbs, R. H. *J. Am. Chem. Soc.* **1986**, *108*, 6402.

(45) (a) Trepanier, S. J.; McDonald, R.; Cowie, M. *Organometallics* **2003**, *22*, 2638. (b) Rowsell, B. D.; McDonald, R.; Cowie, M. *Organometallics* **2004**, *23*, 3873.

(46) (a) Kabir, S. E.; Rosenberg, E.; Stetson, J.; Yin, M.; Ciurash, J.; Mnatsakanova, K.; Hardcastle, K. I.; Noorani, H.; Movsesian, N. *Organometallics* **1996**, *15*, 4473. (b) Cabeza, J.; Franco, R. J.; Llamazares, A.; Riera, V.; Perez-Carreño, E.; Van der Maelen, J. F. *Organometallics* **1994**, *13*, 55. (c) Briard, P.; Cabeza, J.; Llamazares, A.; Ouahab, L.; Riera, V. *Organometallics* **1993**, *12*, 1006. (d) Park, J. W.; Henling, L. M.; Schaefer, W. P.; Grubbs, R. H. *Organometallics* **1991**, *10*, 171.

(47) Mann, B. E.; Taylor, B. F. *^{13}C NMR Data for Organometallic Compounds*; Academic Press: London, U.K., 1981.

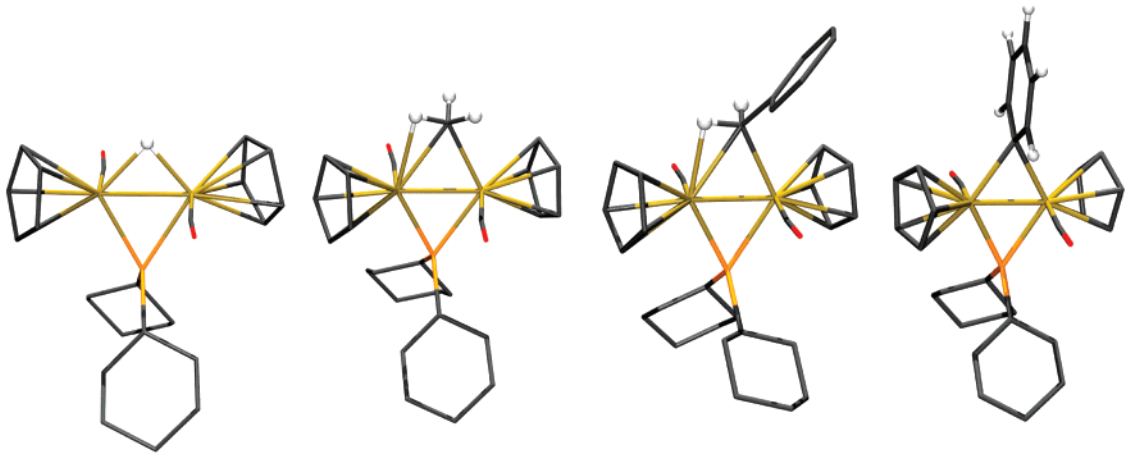

Figure 5. Optimized structures (B3LYP) for compounds **1**−**4**.

same time, the ortho-carbon nuclei give rise to an unusually deshielded resonance at 162.7 ppm. We take these spectroscopic anomalies of **4** as indicative of an unusual interaction of the phenyl bridge with the unsaturated metal center. To this we must add the anomalous ^{31}P chemical shift of this complex (174.8 ppm), significantly higher than those of the agostic complexes **2** and **3** but yet considerably lower than that of the hydride **1**, thus suggesting that the phenyl bridge is not acting as just a one-electron donor. As we will discuss later on, the phenyl bridge in **4** is involved in a π-bonding interaction with the unsaturated dimetal center, thus suggesting a possible origin of the above spectroscopic anomalies.

DFT Calculations on Compounds 1−4. Equilibrium Geometries. The great computational efficiency and chemical accuracy of the DFT methods currently allows ab initio calculations of real (rather than model) transition metal complexes of the size of the binuclear compounds here discussed.[48] We have thus carried out DFT calculations on compounds **1**−**4** (see Experimental Section for further details). Besides, to get a better understanding of the intermetallic interaction in all these substrates, we have carried out similar calculations on the hypothetical anion $[Mo_2Cp_2(\mu\text{-}PCy_2)(CO)_2]^-$ (**A**) resulting from removal of a proton from the hydride **1** while keeping the carbonyl ligands fixed at the terminal positions found in the hydride. This does not correspond to the actual structure of this anion, which has two bridging carbonyls instead.[1]

The optimized geometries for compounds **1**−**4** are in good agreement with those determined by X-ray diffraction (Figure 5). The most relevant bond lengths and angles, both calculated (using the B3LYP and B3PW91 functionals) and experimental (where available), are collected in Table 3. In general, the B3PW91 functional gave the best approach to the experimental parameters, but the differences were not important in any case.

The optimized geometry for the hydride **1** deserves no comments. In the case of the benzyl complex **3**, both the significantly different Mo−C bond distances and the short Mo2−H58 separation calculated indeed support the presence of an agostic C−H···Mo interaction in this molecule. As for the methyl complex **2**, even when the geometry optimization was performed starting from a symmetrical methyl coordination of type I, the structure converged to a point where the Mo1−C and Mo2−C separations were significantly different (as found for **3**) and the Mo2−H46 separation became considerably shortened, as found in the crystal. This supports the presence of an agostic interaction also for this molecule, which is in agreement with the spectroscopic data available for this methyl complex in solution, as discussed in the preceding sections. The calculated asymmetry of the bridgehead carbon is higher for

Table 3. Selected Geometric Parameters of the Optimized and Experimental Structures of Compounds 1 to 4 and A[a]

	B3LYP	B3PW91	X-ray
	Compound **1**		
Mo1−Mo2	2.535	2.535	2.528(2)
Mo1−H	1.861	1.861	1.84(8)
Mo2−H	1.861	1.861	1.88(9)
Mo1−P	2.430	2.430	2.386(3)
Mo2−P	2.430	2.430	2.383(3)
	Compound **2**		
Mo1−Mo2	2.574	2.560	2.558(2)
Mo1−C	2.315	2.287	2.28(1)
Mo2−P	2.430	2.414	2.382(2)
Mo1−P	2.435	2.421	2.384(1)
Mo2−H46	2.298	2.238	2.27(5)
Mo2−C	2.431	2.408	2.43(1)
C−H46	1.105	1.110	0.98(2)
C−H40	1.094	1.094	0.95(2)
C−H47	1.091	1.091	0.96(2)
C−H46−Mo2	83.30	84.87	87(6)
Mo1−C−H46	132.98	131.66	135(6)
	Compound **3**		
Mo1−Mo2	2.587	2.574	2.580(1)
Mo1−C	2.342	2.310	2.294(7)
Mo1−P	2.439	2.421	2.395(2)
Mo2−P	2.438	2.423	2.406(2)
Mo2−H58	2.146	2.103	2.06(5)
Mo2−C	2.484	2.450	2.416(7)
C−H58	1.114	1.120	1.03(6)
C−H49	1.096	1.096	1.01(7)
C−H58−Mo2	93.93	93.98	97(3)
Mo1−C−H58	124.26	124.28	124(3)
	Compound **4**		
Mo1−Mo2	2.577	2.561	2.557(2)
Mo1−C	2.333	2.310	2.31(1)
Mo2−C	2.333	2.310	2.39(1)
Mo1−P	2.429	2.415	2.396(3)
Mo2−P	2.429	2.415	2.386(3)
	Compouind **A**		
Mo1−Mo2	2.432		
Mo1−P	2.426		
Mo2−P	2.426		
Mo1−P−Mo2	60.15		

[a] Selected bond lengths (Å) and angles (deg.) according to the labels of Table 1. The agostic hydrogen atoms are labeled as H46 (**2**) and H58 (**3**).

(48) (a) Koch, W.; Holthausen, M. C. *A Chemist's Guide to Density Functional Theory*, 2nd ed.; Wiley-VCH: Weinheim, Germany, 2002. (b) Ziegler, T. *Chem. Rev.* **1991**, *91*, 651. (c) Foresman, J. B.; Frisch, Æ. *Exploring Chemistry with Electronic Structure Methods*, 2nd ed.; Gaussian: Pittsburgh, PA, 1996.

the benzyl complex **3** (Δd = 0.14 Å) than for the methyl compound **2** (Δd = 0.12 Å), which is suggestive of a stronger agostic interaction in the former case, in agreement with the available spectroscopic data in solution (specially the J_{CH} values), and also consistent with the natural bond orbital (NBO) analysis to be discussed later on. We note here that the DFT optimized geometry of the complex [$Mo_2Cp^*_2(\mu$-Me)(μ-PMe_2)(μ-$O_2CMe)_2$] displays a more asymmetric agostic methyl bridge (Δd = 0.22 Å),[11] even when the complex was found to exhibit a symmetric bridge in the solid state.[17] It seems then that the energetic difference between the agostic and nonagostic coordination modes of the methyl ligand in these unsaturated dimolybdenum complexes is rather small, in agreement with the dynamic behavior of compounds **2** and **3**, and the modest energetic difference computed for the structures **3-I** and **3-II**, as discussed above.

The optimized geometry of complex **4** with B3LYP and B3PW91 density functionals reveals a symmetrical η^1-coordination of the phenyl ring (Mo−C, ca. 2.32 Å) rather than the slightly asymmetric positioning found in the crystal. Moreover the angle between the phenyl ring and the $Mo_2P(\mu$-C) plane is not far from 90° (ca. 112°), thus excluding the possibility that the phenyl group is taking part in an agostic interaction via the ortho hydrogen atoms. Actually, this angle corresponds to a positioning of the ring almost parallel to the Mo−C−O vectors, this minimizing the steric repulsions in the bridging region. Interestingly, the C−C distances within the ring are slightly different, so that the C_{ipso}−C_{ortho} lengths (1.430 Å) are slightly longer than the others (1.408 ± 0.001 Å). This is in agreement with the presence of some π-donation from the ring to the unsaturated dimolybdenum center, as it will be discussed later on.

It is interesting to compare the geometric differences between the anion **A** and the neutral derivatives **1**−**4**, the latter corresponding to the addition of simple electrophiles (H^+, CH_3^+, CH_2Ph^+, Ph^+) to the electron-rich dimetal center of the anion. The main structural change concerns the intermetallic length, which increases from 2.432 Å in anion **A** (B3LYP) up to 2.535 (H), 2.574 (Me), 2.577 (Ph), and 2.587 Å (CH_2Ph). This is in agreement with the qualitative description of the formation of these molecules, whereby a metal−metal bonding pair in the anion combines with the appropriate empty orbital of the electrophile to yield a 3c−2e bonding interaction in the neutral product, a matter to be discussed in more detail later on.

Molecular Orbitals of Compounds A and 1. Molecular orbital theory is the most widely used tool for studying the chemical bond in molecules.[49,50] In the DFT-based framework, Kohn−Sham (KS) orbitals can be used for the analysis of chemical bonding in a way similar to that of the classical MO's, at least in a qualitative way.[49] Accordingly, a detailed analysis of the corresponding KS orbitals has been performed to obtain information about the bonding in our unsaturated molecules.

The upper occupied orbitals both for the anion **A** and the hydride **1** are directly related to the intermetallic interaction and are collected in Figure 6, along with their associated energy and prevalent bonding character. In the anion, a frontier configuration of the type $\pi^2\sigma^2\delta^2\pi^2\delta^{*2}$ results, which gives support to the formulation of the triple metal−metal bond that follows from the application of the EAN rule; now, this triple bond can be more precisely described as having one σ and two π components. When going from the anion **A** to the hydride **1**, a general stabilization of all MO's takes place, but the most significant change is the distinctively strong stabilization of one of the π components of the metal−metal bond in the anion (HOMO-1), which becomes (by combination with the empty 1s orbital of the proton) the tricentric (Mo_2H) orbital holding the hydrogen atom at the bridging position (HOMO-15). At such

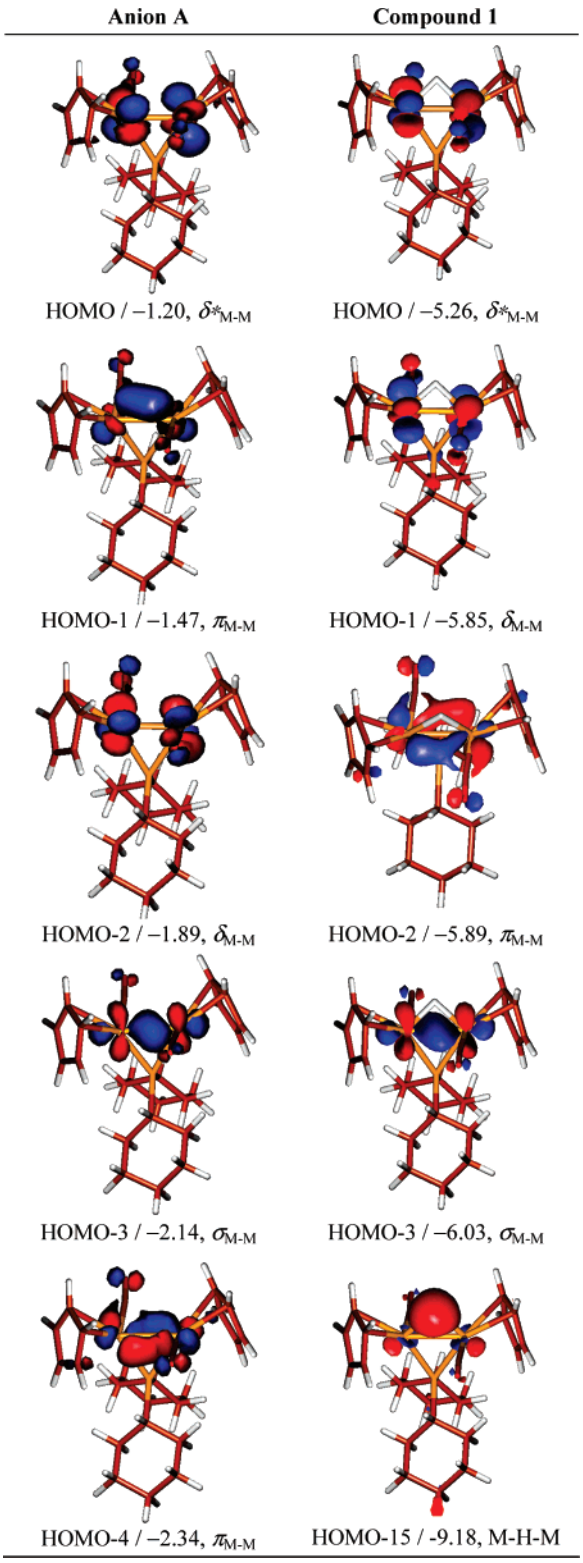

Figure 6. Selected molecular orbitals for compounds **A** and **1**, with their energy (eV) and dominant character shown below.

(49) Cramer, C. J. *Essentials of Computational Chemistry*, 2nd ed.; Wiley: Chichester, U.K., 2004.

(50) (a) Jean, Y. *Molecular Orbitals of Transition Metal Complexes*; Oxford University Press: Oxford, U.K., 2005. (b) Jean, Y.; Volatron, F.; Burdett, J. *An Introduction to Molecular Orbitals;* Oxford University Press: Oxford, U.K., 1993.

a short intermetallic separation as ca. 2.50 Å, there is little doubt that this orbital has both Mo−H and Mo−Mo bonding character. Thus, the intermetallic binding can be described as being composed of a tricentric (Mo_2H) plus two bicentric (Mo_2) interactions, the latter being of σ (HOMO-3) and π (HOMO-2) types, respectively. All this is consistent with the moderate lengthening (0.103 Å at B3LYP level) of the internuclear separation upon protonation of **A** and also with the chemical behavior of the hydride **1**.[2]

The nature of the tricentric bonding interaction present in H-bridged M−M bonds of the transition metal complexes has been the subject of considerable attention and controversy over the years.[11] As stated in the introductory section, earlier calculations at different levels on electron-deficient di- or polyhydride complexes having a central $M_2(\mu\text{-H})_x$ moiety had led to the conclusion that essentially no direct metal−metal bonding results from the tricentric M−H−M interactions there present,[10,11] and a similar conclusion was more recently reached using DFT calculations on the model molybdenum(III) hydride complex $[Mo_2Cp_2(\mu\text{-H})(\mu\text{-PH}_2)(\mu\text{-O}_2\text{CH})_2]$ (yet the orbital interaction relating this hydride complex with its anionic precursor is essentially identical to that in the pair **A**/**1**).[11] While we trust that the absence of any direct M−M bonding interaction might be taken for granted at very large intermetallic separations, as shown also by the detailed DFT calculations carried out recently on the electron-precise hydride $[Cr_2(\mu\text{-H})(CO)_{10}]^-$,[51] tricentric M−H−M bonds at very short intermetallic separations most probably retain significant direct M−M bonding interaction. In line with this view, a very recent DFT study on the single and double protonation products of model Fe_2 and Ir_2 complexes having double M−M bonds has also concluded that in the protonated species there is significant M−M bonding, although the strength of the interaction decreases when the bond is protonated.[52] In the other extreme, ignoring completely the M−M bonding interaction implied in the tricentric M−H−M bonds would make the hydride ligand equivalent to a three-electron donor such as the chloride or dialkylphosphide bridging ligands (concerning to the intermetallic interaction). In the case of the hydride **1**, this would imply assimilation of this 30-e complex to the 32-e complexes $[Mo_2Cp_2(\mu\text{-X})(\mu\text{-PCy}_2)(CO)_2]$ (X = Cl,[1] PRR′),[25] a relationship of little use in interpreting the strong differences separating the structure, spectroscopic properties, and reactivity of these molecules.

Molecular Orbitals of the Hydrocarbyl Complexes 2−4. The upper occupied orbitals for these compounds are collected in Figure 7, along with their associated energy and prevalent bonding character. In general, these orbitals are similar to those of the hydride **1**, although a more extensive orbital mixing occurs, and there are also some interesting differences. First, a frontier configuration of the type $\sigma^2\pi^2\delta^2\delta^{*2}$ is obtained in all cases, accounting for the presence of two bicentric Mo−Mo bonding interactions with σ and π character, respectively, as found for **1**. Besides, the tricentric M−H−M orbital found for **1** is here replaced by a strongly stabilized tricentric M−C−M orbital [HOMO-13 (**2**), HOMO-14 (**3**), and HOMO-15 (**4**)]. This would lead us to a description of the intermetallic interaction in these hydrocarbyl bridged complexes quite similar to that discussed for the hydride **1**, it being made up of a tricentric (Mo_2C) plus two bicentric (Mo_2) interactions, the latter being of σ and π types, respectively. However, we can indentify additional interactions reducing the strength of the intermetallic binding. In the case of the methyl complex, no clear indication for the presence of the agostic C−H···Mo interaction can be obtained by inspection of the orbitals, but in the benzyl complex **3** such an interaction can be clearly appreciated by inspection of the HOMO-4, which, while having dominant σ_{MM} character, yet represents a bonding C−H···M interaction reminiscent of that calculated for $[Fe_2Cp_2(\mu\text{-CH}_3)(\mu\text{-CO})(CO)_2]^+$ by the Fenske−Hall method.[9] Such an interaction is detrimental for the σ_{MM} bond and thus implies a weakening of the intermetallic binding, in agreement with the progressive increase of the internuclear separations in the order **1** < **2** < **3**. For the phenyl complex **4**, the HOMO-9 denotes the presence of a π-donor interaction from the π-bonding orbitals of the hydrocarbon ring into suitable metal acceptor orbitals. Such an interaction reinforces the Mo−C bond (recall the relatively short Mo−C lengths and the calculated lengthening of the $C_{ipso}-C_{ortho}$ bonds), while weakening the Mo−Mo bond (hence the lengthening relative to **1**), because of the antibonding character with respect to the M−M overlap. To our knowledge, this sort of π-donor interaction of a bridging η^1-phenyl ligand has not been previously recognized in a MO analysis.

In summary, at least for the benzyl complex **3** and for the phenyl complex **4** we can identify orbital interactions that make these bridging ligands to effectively contribute to the dimetal center with more than one electron, thus reducing the strength of the intermetallic binding. The geometrical parameters of these complexes suggest that those interactions do not imply the additional involvement of a full electron pair, then making the bridging ligand a three-electron donor group (Chart 1), but the interaction goes indeed in that direction. Our orbital analysis, however, does not give us the strength of these bonding contributions, a question that we have addressed using data derived from the AIM and NBO analyses of these complexes.

AIM Analysis of the Bonding in Compounds 1−4. The properties of the electron density in complexes **A** and **1**−**4** at selected (3, −1) bond critical points (BCP) and (3, +1) ring critical points (RCP) calculated with the B3LYP density functional are summarized in Table 4, and pictures of the charge density in the Mo_2P plane for compounds **1**−**4** are shown in Figure 8. Compounds **1** and **4** exhibit a similar topology of the electron density at their bridging region. Note, however, the inward deformation of the Mo−H bond paths, characteristic of 3c−2e interactions, while the Mo−C bond paths of **4** are almost straight lines. This is in agreement with the presence of interactions (π-donation) additional to the tricentric Mo_2C bond which reinforce the Mo−C bonds as suggested by the previous MO analysis.

In the case of the alkyl complexes **2** and **3**, a key question is the independent detection of the agostic interaction (suggested by the geometrical features) from the features of the topology of the electron density. Previous AIM analysis of β-agostic interactions in mononuclear complexes reveal that the main topological characteristic of such interactions is the appearance of a bond path (and the corresponding BCP) connecting the corresponding metal and H (but not C) atoms.[8] This feature is not observed in our alkyl compounds. For the methyl complex **2**, bond paths connecting the bridging C atom to both metal centers are found, but that with the metal atom engaged in the agostic interaction is severely bent inward, so that the corresponding BCP is very close to the critical point of the Mo_2C ring, which is consistent with incipient rupture of that Mo−C bond (note the low value of ρ at that BCP). In fact this is what we find for the benzyl complex **3**, lacking the Mo−C bond path to the metal engaged in the agostic interaction. Yet, the expected

(51) Macchi, P.; Donghi, D.; Sironi, A. *J. Am. Chem. Soc.* **2005**, *127*, 16494.

(52) Phillips, A. D.; Ienco, A.; Reinhold, J.; Bötcher, H. C.; Mealli, C. *Chem. Eur. J.* **2006**, *12*, 4691.

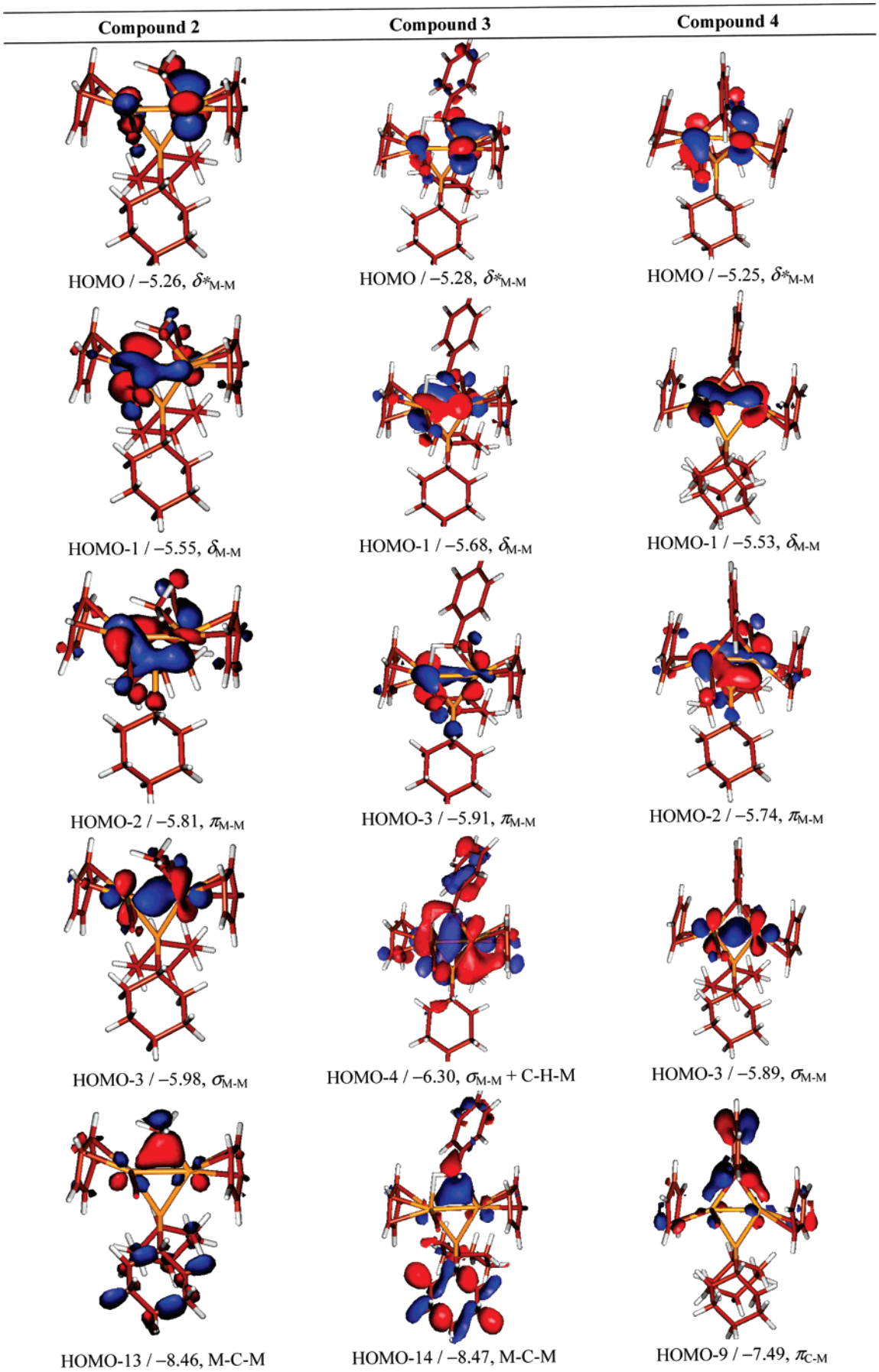

Figure 7. Selected molecular orbitals for compounds **2**−**4**, with their energy (eV) and dominant character shown below.

bond path connecting that metal atom (Mo2) and the agostic hydrogen (H58) is absent. These features persisted for either **2** or **3** even when using the more complete SSD basis set for the molybdenum atoms (see Experimental Section), then pointing

Table 4. Topological Properties of the Electron Density at the Bond Critical Points[a]

	A		1		2		3		4	
bond	ρ	$\nabla^2\rho$	ρ	$\nabla^2\rho$	ρ	$\nabla^2\rho$	ρ	$\nabla^2\rho$	ρ	$\nabla^2\rho$
Mo1−Mo2	0.684	0.82	0.582	0.52	0.538	0.42	0.530	0.39	0.537	0.41
Mo1−P	0.517	0.96	0.535	0.79	0.535	0.77	0.530	0.76	0.542	0.75
Mo2−P	0.517	0.96	0.535	0.79	0.545	0.74	0.536	0.72	0.542	0.75
Mo1−X			0.532	1.18	0.482	0.91	0.475	0.82	0.456	1.01
Mo2−X			0.532	1.18	0.363	0.72			0.456	1.01
X−Hag					1.735	−4.73	1.707	−4.56		
X−H					1.809	−5.16	1.836	−5.29		
					1.838	−5.34				
X−C							1.663	−3.36		

[a] Values of the electron density at the bond critical points (ρ) are given in e Å^{-3}; values of the laplacian of the electron density at these points ($\nabla^2\rho$) are given in e Å^{-5}; Mo labels according to the figures of Table 1; X = H (**1**) or C (**2**−**4**).

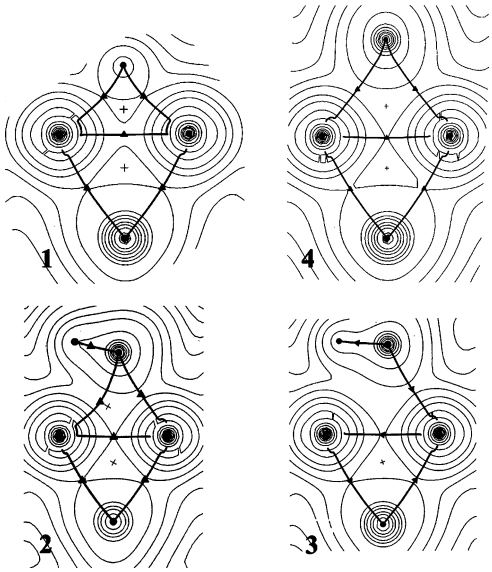

Figure 8. Contour lines of the electron density (B3LYP) in the plane Mo_2P of compounds **1**−**4**, showing the bond paths linking the bond critical points (▲) and the corresponding atoms (●), as well as the ring critical points (×).

to a genuine result, which might be the consequence of the weakness of the agostic interaction. In fact, it has been reported that M−H bond paths and their corresponding BCP may not always be found in molecules having agostic interactions.[8b,c] We note, however, that there is a slight reduction of ca. 0.1 e Å^{-3} in the electron density at the BCP of the agostic C−H bonds in these complexes (compared to the nonagostic bonds), as expected.

From the orbital analysis made above, it is clear that the triple metal−metal bond present in anion **A** is substantially weakened upon protonation, due to the conversion of a π_{MM} bond into a tricentric Mo_2H bond. This effect must be more pronounced in the formation of alkyls **2** and **3** or phenyl complex **4**, due to the appearance of additional bonding interactions, α-agostic and π-donor, respectively. All this is reflected in the progressive reduction of electron density at the intermetallic BCPs, 0.684 (**A**) > 0.582 (**1**) > 0.538 (**2**) ∼ 0.537 (**4**) > 0.530 (**3**) e Å^{-3}, and similar trends are observed for the laplacian of the electron density. The above figures confirm the higher strength of the agostic interaction for the benzyl complex, relative to its methyl analogue, in line with their distinct bond paths and orbital features already discussed. These figures also suggest that the π-donor interaction of the phenyl ring is of effective strength similar to that of the α-agostic interaction in the methyl complex, which is what we would have anticipated on the basis of their almost identical calculated intermetallic separations. Yet, the significant difference in their ^{31}P NMR chemical shifts in solution (153.3 ppm for **2** vs 174.8 ppm for **4**) obviously does not have a geometrical origin and cannot be explained easily.

A further procedure for estimating the amount of direct M−M interaction remaining in a tricentric M_2H or related interaction at short intermetallic distances would be to compare the electronic properties at the intermetallic BCP with those of isoelectronic complexes displaying similarly short M−M separations and lacking those tricentric interactions. Although these data are yet very scarce, we can quote here that very recent DFT calculations carried out by us at similar levels of theory on the 30-electron carbonyl- and methoxycarbyne-bridged complexes of the type $[Mo_2Cp_2(\mu\text{-}PR_2)_x(\mu\text{-}COMe)_y(\mu\text{-}CO)_z]^n$ (x + y + z = 3; $n = -1, 0, +1$), displaying intermetallic distances in the range 2.499−2.537 Å, gave electron densities at the intermetallic BCPs in the range of 0.584−0.615 e Å^{-3}, actually not far from that calculated for the triply bonded complex $[Mo_2Cp_2(CO)_4]$ (0.576 e Å^{-3}).[53] The latter comparison is of relevance since this tetracarbonyl complex only displays linear semibridging carbonyls and no other bridges. Yet, the electron density at the intermetallic BCP is almost the same as that in the hydride-bridged **1** (0.582 e Å^{-3}). These comparisons reinforce our idea that the tricentric Mo_2H and Mo_2C bonds present in complexes **1**−**4** retain substantial direct M−M bonding character, possibly facilitated by the very short intermetallic separations.

Estimation of the Strength of the Agostic and π-Bonding Interactions by NBO Analysis. Natural bond orbital analysis[54] was performed in order to gain complementary insight into the nature of the Mo−Mo interactions in all compounds, as well as the additional interactions present in the hydrocarbyl complexes **2**−**4**. The results of this analysis are summarized in Table 5. As expected, two direct Mo−Mo bonding pairs are found for compounds **1**−**4**, and three in the case of anion **A**, which exhibits the highest Wiberg (1.44) and Mayer (1.69) indexes. These indexes then decrease in the sequence **1** > **2** ∼ **4** > **3**, thus paralleling the sequence of the electron densities at the intermetallic BCP found in the AIM analysis. The gap in the indexes between hydride **1** and hydrocarbyl complexes **2**−**4** is considered as an effect of the additional (α-agostic and π-donor) interactions present in the latter. Further evidence for the presence of the above additional interactions can be obtained in the agostic complexes through the *W* or *M* indexes of the agostic C−H bonds in complexes **2** and **3**, which have values of ca. 0.05 (**2**) and 0.1 (**3**) below those of the corresponding nonagostic C−H bonds. Also very small but nonzero *W* indexes of 0.03 (**2**) and 0.05 (**3**) can be calculated for the corresponding Mo···H interactions. However, a better and more quantitative description of the α-agostic interaction in the alkyl complexes

(53) García, M. E.; García-Vivó, D.; Ruiz, M. A.; Alvarez, S.; Aullón, G. *Organometallics* **2007**, *26*, 4930.

(54) (a) Reed, A. E., Curtiss, L. A., Weinhold, F., *Chem. Rev.* **1988**, *88*, 899. (b) Foster, J. P.; Weinhold, F. *J. Am. Chem. Soc.* **1980**, *102*, 7211.

Table 5. Properties of Selected NBOs[a]

	A		**1**		**2**		**3**		**4**	
bond	W	M	W	M	W	M	W	M	W	M
Mo1−Mo2	1.44	1.69	0.97	1.27	0.80	1.06	0.77	1.04	0.80	1.07
Mo1−P	0.77	0.78	0.78	0.82	0.74	0.81	0.74	0.79	0.74	0.82
Mo2−P	0.77	0.78	0.78	0.82	0.75	0.81	0.74	0.80	0.74	0.80
Mo1−X			0.37	0.46	0.48	0.62	0.47	0.51	0.41	0.44
Mo2−X			0.37	0.46	0.34	0.37	0.29	0.41	0.41	0.44
X−Hag					0.87	0.81	0.82	0.75		
X−H					0.91	0.86	0.92	0.87		
					0.94	0.88				
X−C							1.06	0.96		

[a] Mo labels according to the figures of Table 1; X = H (**1**) or C (**2**−**4**); W = Wiberg index; M = Mayer index (see Experimental Section).

Table 6. Second-Order Perturbation Analysis for Selected Interactions[a]

		energy/(kJ mol^{-1})		
donor	acceptor	**2**	**3**	**4**
BD(Mo1−X)	LP*(Mo2)	277.1	221.8	340.5
CR(X)	LP*(Mo2)	18.5	15.4	22.0
BD(X−H_{ag})	LP*(Mo2)	70.3	89.2	
C−X[b]	LP*(Mo2)			25.6 24.6

[a] Mo labels according to the figures of Table 1; X = C; BD = bond; LP = lone pair; CR = core. [b] Bonding pairs of the C_{ipso}−C_{ortho} bonds.

2 and **3** can be obtained by the second-order perturbation analysis that provides the energy of interaction between donor and acceptor NBOs (Table 6). In both cases, one of the C−H bonds is able to act as a donor to an empty lone pair on one molybdenum atom, this accounting for a stabilization energy of 70.3 (**2**) and 89.2 (**3**) kJ mol^{-1}, respectively, in agreement with the geometric parameters that suggest a stronger agostic interaction for the benzyl complex. We can compare the above figures with the value of ca. 73 kJ mol^{-1} recently calculated using the same methodology for the linear agostic C−H···Ta interaction present in the mononuclear model complex $[TaCl_3(OC_6H_4)_3CH\}]^-$.[55] As far as the phenyl complex is concerned, the perturbation analysis suggests that there are weak interactions between the C_{ipso}−C_{ortho} bonds and an empty lone pair on molybdenum, these adding up to 52.2 kJ mol^{-1}. This gives support to the expectations based on the geometrical parameters of all these complexes, which suggest that the π-donor interaction of the phenyl ring in **4** is of comparable strength to the weak agostic interaction present in the methyl complex **2**.

Conclusions

DFT calculations (B3LYP, B3PW91) correctly reproduce the experimental structures of hydride **1** and hydrocarbyl-bridged complexes **2**−**4** and predict α-agostic geometries for both the methyl and benzyl complexes, in agreement with the solution and solid-state data. For the benzyl complex **3**, the agostic structure is estimated to be only ca. 34 kJ mol^{-1} more stable than the nonagostic structure, thus enabling their coexistence in solution, as it is proposed to explain the dynamic behavior of this complex. The intermetallic binding in the hydride complex can be described as composed of a tricentric (Mo_2H) plus two bicentric (Mo_2) interactions, the latter being of σ and π types. In the hydrocarbyl-bridged complexes, analogous tricentric (Mo_2C) and bicentric (Mo_2) interactions can be identified, but there are additional interactions reducing the strength of the intermetallic binding. These are the α-agostic bonding in the case of the alkyl complexes and a π-donor interaction from the π-bonding orbitals of the hydrocarbon ring into suitable metal acceptor orbitals, in the case of the phenyl complex. The stabilization energy of these additional interactions have been estimated by second-order perturbation analysis to be of 70.3 (Me), 89.2 (CH_2Ph), and 52.2 (Ph) kJ mol^{-1}, respectively. The AIM analysis fails to detect the expected bond paths connecting the agostic hydrogen and the corresponding metal atom in the methyl and benzyl complexes, due to the weakness of such interactions, but correctly predicts the expected reductions of electron density at the corresponding C−H and Mo−Mo bonds. The electron densities at the intermetallic BCPs remain quite high in these hydrocarbyl-bridged complexes, only ca. 0.05 e Å^{-3} below the value for the hydride-bridged **1** (0.582 e Å^{-3}). The latter value is in turn only ca. 0.1 e Å^{-3} lower than that at the pure triple bond present in the anion **A** with an imposed geometry of terminal carbonyls (0.684 e Å^{-3}), and moreover it is a value comparable to those calculated for related 30-electron complexes having no hydride bridges.

Experimental Section

General Procedures and Starting Materials. All manipulations and reactions were carried out under a nitrogen (99.995%) atmosphere using standard Schlenk techniques. Solvents were purified according to literature procedures and distilled prior to use.[56] Tetrahydrofuran solutions of $Li[Mo_2Cp_2(\mu\text{-}PCy_2)(\mu\text{-}CO)_2]$ were usually prepared in situ as described previously,[1] and all other reagents were obtained from the usual commercial suppliers and used as received, unless otherwise stated. Petroleum ether refers to that fraction distilling in the range of 338−343 K. Chromatographic separations were carried out using jacketed columns cooled by tap water (ca. 288 K) or by a closed 2-propanol circuit, kept at the desired temperature with a cryostat. Commercial aluminum oxide (activity I, 150 mesh) was degassed under vacuum prior to use. The latter was mixed under nitrogen with the appropriate amount of water to reach the activity desired. IR stretching frequencies of CO ligands were measured in CaF_2 windows for solutions and are referred to as ν(CO). Nuclear magnetic resonance (NMR) spectra were routinely recorded at 300.13 (^{1}H), 121.50 (^{31}P-$\{^1$H$\}$), or 75.47 MHz (^{13}C$\{^1$H$\}$) at 290 K in CD_2Cl_2 solutions unless otherwise stated. Chemical shifts (δ) are given in ppm, relative to internal tetramethylsilane (^{1}H, ^{13}C) or external 85% aqueous H_3PO_4 solutions (^{31}P). Coupling constants (J) are given in hertz.

Preparation of $[Mo_2Cp_2(\mu\text{-}H)(\mu\text{-}PCy_2)(CO)_2]$ (1). Solid $[NH_4][PF_6]$ (0.325 g, 2.0 mmol) was added to a tetrahydrofuran solution (20 mL) of $Li[Mo_2Cp_2(\mu\text{-}PCy_2)(\mu\text{-}CO)_2]$, prepared in two steps from $[Mo_2Cp_2(CO)_6]$ (0.500 g, 1.02 mmol), $ClPCy_2$ (300 μL, 1.22 mmol), and then 1 M $Li[BHEt_3]$ (3 mL of a 1 M solution in THF, 3 mmol)

(55) Chaplin, A. B.; Harrison, J. A.; Nielson, A. J.; Shen, C.; Waters, J. M. *Dalton Trans.* **2004**, 2643.

(56) Perrin, D. D.; Armarego, W. L. F. *Purification of Laboratory Chemicals*; Pergamon Press: Oxford, U.K., 1988.

as described previously,[1] and the mixture was stirred for 5 min to give a dark brown solution. Solvent was then removed under vacuum, and the residue was washed with acetonitrile (3 × 10 mL) and then chromatographed on alumina (activity IV) at 253 K. Elution with dichloromethane−petroleum ether (1:4) gave a brown fraction which yielded, after removal of solvents, compound **1** (0.405 mg, 69% overall yield) as a brown powder. Anal. Calcd for $C_{24}H_{33}Mo_2O_2P$: C, 49.65; H, 5.73. Found: C, 49.79; H, 6.37. ^{1}H NMR: δ 5.09 (s, 10H, Cp), 2.60−0.85 (m, 22H, Cy), −6.94 (d, J_{PH} = 11, 1H, μ-H). ^{13}C{^{1}H} NMR (50.32 MHz): δ 248.5 (d, J_{CP} = 14, CO), 88.3 (s, Cp), 49.0 (d, J_{CP} = 18, C^1−Cy), 34.1, 33.3 (2 x s, br, C^{2,6}−Cy), 28.1 (d, J_{CP} = 11, C^{3,5}−Cy), 26.4 (s, C^4−Cy). Variable-temperature data (only cyclohexyl resonances given). ^{13}C-{^{1}H} NMR (tol-d_8, 100.63 MHz, 298 K): δ 49.9 (d, J_{CP} = 17, C^1), 35.1, 34.0 (2 × s, C^{2,6}), 28.9 (d, J_{CP} = 12, C^{3,5}), 28.8 (d, J_{CP} = 10, C^{5,3}), 27.2 (s, C^4). ^{13}C{^{1}H} NMR (tol-d_8, 100.63 MHz, 368 K): δ 50.9 (d, J_{CP} = 16, C^1), 35.0 (s, C^{2,6}), 29.2 (d, J_{CP} = 11, C^{3,5}), 27.4 (s, C^4). ^{13}C{^{1}H} NMR (100.63 MHz, 253 K): δ 48.0 (d, J_{CP} = 17, C^1), 33.9, 32.5 (2 × s, C^{2,6}), 27.8 (d, J_{CP} = 13, C^{3,5}), 27.5 (d, J_{CP} = 10, C^{5,3}), 26.0 (s, C^4−Cy). ^{13}C{^{1}H} NMR (100.63 MHz, 213 K): δ 47.5 (s, br, C^1), 34.1, 32.2 (2 × s, C^{2,6}), 27.9 (d, J_{CP} = 13, C^{3,5}), 27.6 (d, J_{CP} = 10, C^{5,3}), 26.2 (s, C^4). ^{13}C{^{1}H} NMR (100.63 MHz, 188 K): δ 34.2 (s, C^{2,6}), 31.9 (s, br, C^{6,2}), 26.1 (s, C^4); the signal due to the C^1 nuclei has disappeared into the noise of the baseline at this temperature.

Preparation of [Mo$_2$Cp$_2$(μ-CH$_3$)(μ-PCy$_2$)(CO)$_2$] (2). Neat CH_3I (0.2 mL, 3.2 mmol) was added to a THF solution (20 mL) of Li[Mo$_2$Cp$_2$(μ-PCy$_2$)(μ-CO)$_2$], prepared from [Mo$_2$Cp$_2$(CO)$_6$] (0.500 g, 1.02 mmol), ClPCy$_2$ (300 μL, 1.22 mmol), and then 1 M Li[BHEt$_3$] (3 mL of a 1 M solution in THF, 3 mmol) as described previously,[1] and the mixture was stirred for 2 h to give a brown solution containing **2** and small amounts of [Mo$_2$Cp$_2$(μ-I)(μ-PCy$_2$)-(CO)$_2$]. The solvent was then removed under vacuum, the residue was extracted with dichloromethane−petroleum ether (1:8) and the extracts were chromatographed on alumina (activity II) at 243 K. Elution with the latter mixture gave a brown fraction and then a green fraction. Removal of solvents from these solutions gave respectively compound **2** as a brown powder (0.385 g, 63% overall yield) and complex [Mo$_2$Cp$_2$(μ-I)(μ-PCy$_2$)(CO)$_2$] as a green solid (0.035 g, 5% overall yield). The crystals used in the X-ray study of **2** were grown by slow diffusion of a layer of petroleum ether into a concentrated toluene solution of the complex at 253 K. Anal. Calcd for $C_{25}H_{35}Mo_2O_2P$: C, 50.86; H, 5.98. Found: C, 50.68; H, 5.35. ^{1}H NMR: δ 5.16 (s, 10H, Cp), 2.30−1.10 (m, 22H, Cy), −0.77 (d, J_{PH} = 2.5, J_{CH} = 124, 3H, μ-CH$_3$). ^{13}C{^{1}H} NMR (100.63 MHz): δ 249.6 (d, J_{CP} = 15, CO), 89.4 (s, Cp), 47.0 (d, J_{CP} = 18, C^1−Cy), 34.2 (d, J_{CP} = 3, C^{2,6}−Cy), 33.1 (s, C^{6,2}−Cy), 28.4 (d, J_{CP} = 13, C^{3,5}−Cy), 28.2 (d, J_{CP} = 11, C^{5,3}−Cy), 26.5 (s, C^4−Cy), −44.3 (d, J_{CP} = 3, μ-CH$_3$).

Preparation of [Mo$_2$Cp$_2$(μ-CH$_2$Ph)(μ-PCy$_2$)(CO)$_2$] (3). Neat $PhCH_2Cl$ (0.5 mL, 4.3 mmol) was added to a THF solution (20 mL) of Li[Mo$_2$Cp$_2$(μ-PCy$_2$)(μ-CO)$_2$] prepared in two steps from [Mo$_2$Cp$_2$(CO)$_6$] (0.500 g, 1.02 mmol), ClPCy$_2$ (300 μL, 1.22 mmol), and then 1 M Li[BHEt$_3$] (3 mL of a 1 M solution in THF, 3 mmol) as described previously,[1] and the mixture was stirred for 18 h to give a brown solution. Solvent was then removed under vacuum, the residue extracted with dichloromethane−petroleum ether (1:8) and the extracts were chromatographed on alumina (activity IV). Elution with the same solvent mixture gave a brown fraction yielding, after removal of solvents, compound **3** as a brown powder (0.330 g, 49% overall yield). The crystals used in the X-ray study of **3** were grown by slow diffusion of a layer of petroleum ether into a concentrated toluene solution of the complex at 253 K. Anal. Calcd for $C_{31}H_{39}Mo_2O_2P$: C, 55.86; H, 5.90. Found: C, 55.71; H, 6.45. ^{1}H NMR (200.13 MHz): δ 7.30−6.80 (m, 5H, Ph), 5.17 (s, 10H, Cp), 2.46 (d, J_{HH} = 15, 1H, μ-CH$_2$), 2.30−1.10 (m, 22H, Cy), −1.35 (dd, J_{HH} = 15, J_{PH} = 2, 1H, μ-CH$_2$). Variable temperature data (only Cp and CH$_2$ resonances given): ^{1}H NMR (400.14 MHz, 243 K): δ 5.21 (s, 10H, Cp), 2.68 (d, J_{HH} = 15, 1H, μ-CH$_2$), −1.66 (dd, J_{HH} = 15, J_{PH} = 2, 1H, μ-CH$_2$). ^{1}H NMR (400.14 MHz, 218 K): δ 5.27 (s, br, 10H, Cp), 2.79 (d, J_{HH} = 15, 1H, μ-CH$_2$), −1.75 (d, J_{HH} = 15, 1H, μ-CH$_2$). ^{1}H NMR (400.14 MHz, 193 K): d 5.46, 5.04 (2 × s, 2 × 5H, 2 × Cp), 2.83 (d, J_{HH} = 15, 1H, μ-CH$_2$), −1.88 (d, J_{HH} = 15, 1H, μ-CH$_2$). ^{1}H NMR (tol-d_8, 400.14 MHz, 298 K): δ 4.86 (s, 10H, Cp), 2.42 (d, J_{HH} = 15, 1H, μ-CH$_2$), −1.27 (dd, J_{HH} = 15, J_{PH} = 3, 1H, μ-CH$_2$). ^{1}H NMR (tol-d_8, 400.14 MHz, 338 K): δ 4.90 (s, 10H, Cp), 2.23 (d, J_{HH} = 15, 1H, μ-CH$_2$), −0.99 (dd, J_{HH} = 15, J_{PH} = 3, 1H, μ-CH$_2$). ^{1}H NMR (tol-d_8, 400.14 MHz, 378 K): δ 4.90 (s, 10H, Cp), 2.09 (d, J_{HH} = 15, 1H, μ-CH$_2$), −0.73 (dd, J_{HH} = 15, J_{PH} = 3, 1H, μ-CH$_2$). ^{13}C{^{1}H} NMR: δ 248.0 (d, J_{CP} = 14, CO), 154.0 (s, C^1-Ph), 127.6, 127.2 (2 × s, C^{2,3}−Ph), 121.9 (s, C^4−Ph), 89.5 (s, Cp), 47.0 (d, J_{CP} = 19, C^1−Cy), 33.9 (d, J_{CP} = 4, C^{2,6}−Cy), 32.9 (s, C^{6,2}−Cy), 28.3 (d, J_{CP} = 13, C^{3,5}−Cy), 28.0 (d, J_{CP} = 11, C^{5,3}−Cy), 26.3 (s, C^4−Cy), −4.2 (d, J_{CP} = 2, μ-CH$_2$). ^{13}C NMR: δ -4.2 (dd, J_{CH} = 130, 100, μ-CH$_2$).

Preparation of [Mo$_2$Cp$_2$(μ-Ph)(μ-PCy$_2$)(CO)$_2$] (4). A red solution of Li[Mo$_2$Cp$_2$(μ-PCy$_2$)(μ-CO)$_2$] (ca. 0.07 mmol) in THF (10 mL) was prepared by reacting compound **1** (0.040 g, 0.07 mmol) and Li[BHEt$_3$] (100 μL of a 1 M solution in THF, 0.1 mmol) for 5 min at room temperature. Solvent was then removed under vacuum, and dichloromethane (10 mL) was afterward added to the residue to give a red suspension. Solid Ph_3PbCl (0.050 g, 0.095 mmol) was then added to the latter suspension, and the mixture was stirred for 4 h to give a red solution. Solvent was then removed under vacuum, and the residue was chromatographed on alumina (activity II). Elution with dichloromethane−petroleum ether (1:4) gave a red-brown fraction yielding, after removal of solvents, compound **4** (0.039 g, 85% overall yield) as a red-brown powder. The crystals used in the X-ray study of **4** were grown by slow diffusion of a layer of petroleum ether into a concentrated dichloromethane solution of the complex at 253 K. Anal. Calcd for $C_{30}H_{37}Mo_2O_2P$ (**4**): C, 55.22; H, 5.72. Found: C, 54.84; H, 6.21. ^{1}H NMR ($CDCl_3$): δ 8.58 (false d, apparent J_{HH} = 7, 2H, H^{2-}Ph), 7.73 (tt, J_{HH} = 7, 1.5, 1H, H^4−Ph), 7.03 (false tt, apparent J_{HH} = 7, 1.5, 2H, H^3−Ph), 4.86 (s, 10H, Cp), 2.60−1.20 (m, 22H, Cy). ^{13}C{^{1}H} NMR ($CDCl_3$): δ 252.4 (d, J_{CP} = 16, CO), 162.7 (d, J_{CP} = 1.5, C^{2-}Ph), 132.8 (d, J_{CP} = 1.5, C^4−Ph), 125.8 (d, J_{CP} = 6, C^1−Ph), 121.8 (d, J_{CP} = 1, C^3−Ph), 88.2 (s, Cp), 48.3 (d, J_{CP} = 18, C^1−Cy), 33.6 (d, J_{CP} = 5, C^{2,6}−Cy), 32.8 (d, J_{CP} = 2, C^{6,2}−Cy), 28.1 (d, J_{CP} = 12, C^{3,5}−Cy), 27.9 (d, J_{CP} = 9, C^{5,3}−Cy), 26.2 (d, J_{CP} = 1.5, C^4−Cy).

DFT Calculations. Geometry optimizations for compounds **1**−**4** were performed using initial coordinates derived from X-ray data. A geometry optimization was also performed for the [Mo$_2$Cp$_2$(μ-PCy$_2$)(CO)$_2$]$^-$ anion **A** starting from the initial coordinates of the equilibrium geometry calculated for the hydride **1**, after removal of H$^+$ and fixing the Mo−CO fragments to be linear, in order to better compare the bond properties at the intermetallic region of the anion with those of the neutral complexes. The gradient-corrected hybrid density functionals B3LYP,[57,58] B3PW91,[59] and the double-ζ basis set LANL2DZ with Hay and Wadt effective core potential (ECP)[60] have been employed. Single point energy calculations were performed for all complexes using the B3LYP density functional and the LANL2DZ basis set for the molybdenum atoms and the 6-311+G(d,p) basis set for the remaining atoms in order to obtain good quality wave functions to submit to the AIM analysis. The diffuse and polarization functions of the 6-311+G-

(57) Becke, A. D. *Phys. Rev. A* **1988**, *38*, 3098.
(58) Becke, A. D. *J. Chem. Phys.* **1993**, *98*, 5648.
(59) (a) Perdew, J. P. In *Electronic Structure of Solids*; Ziesche, P., Eschrig, H., Eds.; Akademie Verlag: Berlin, 1991. (b) Perdew, J. P.; Wang, Y., *Phys. Rev. B* **1992**, *45*, 13244.
(60) (a) Hay, P. J.; Wadt, W. R. *J. Chem. Phys.* **1985**, *82*, 299. (b) Wadt, W. R.; Hay, P. J. *J. Chem. Phys.* **1985**, *82*, 284.

Table 7. Crystal Data for Compounds 2−4

	2	3	4
mol formula	$C_{25}H_{35}Mo_2O_2P$	$C_{31}H_{39}Mo_2O_2P$	$C_{28.50}H_{35.75}Cl_{0.25}Mo_2O_2P$
MW	590.38	666.47	642.03
cryst syst	monoclinic	monoclinic	monoclinic
space group	*C*2/*c*	$P2_1/a$	*C*2/*c*
radiation (λ, Å)	0.710 73	0.710 73	0.710 73
a, Å	35.85(3)	10.308(5)	17.751(4)
b, Å	8.899(7)	29.438(10)	10.243(3)
c, Å	15.788(15)	9.913(4)	29.979(8)
α, deg	90	90	90
β, deg	102.58(2)	108.74(2)	93.39(2)
γ, deg	90	90	90
V, Å^3	4916(7)	2849(2)	5441(2)
Z	8	4	8
calcd density, g cm^{-1}	1.595	1.554	1.567
abs coeff., mm^{-1}	1.104	0.963	1.028
temp, K	293(2)	293(2)	293(2)
θ range, deg	3.11 to 29.99	3.00 to 25.00	2.64 to 27.05
index ranges (*h*, *k*, *l*)	−50, 49; 0, 12; 0, 20	−12, 11; 0, 35; 0, 11	−22, 22; −13, 13; −38, 38
no. of reflns collected	7232	5288	21447
no. of indep reflns (R_{int})	7007 (0.0244)	4996 (0.0790)	4561 (0.1764)
no. of reflns with $I > 2\sigma(I)$	4838	2504	1424
R indexes[a] [data with $I > 2\sigma(I)$]			
R_1	0.0330	0.0508	0.1060
R_{w2}	0.0770 [b]	0.0580 [c]	0.2385 [d]
R indexes[a] (all data)			
R_1	0.0585	0.1493	0.1433
R_{w2}	0.0852 [b]	0.0713[c]	0.2641[d]
GOF	1.004	0.816	1.055
no. of restraints/param	6/295	0/333	11/213
$\Delta\rho$(max,min), e Å^{-3}	0.853, −1.239	0.686, −0.664	1.099, −1.063

[a] $w^{-1} = \sigma^2(F_o^2) + (aP)^2 + (bP)$, where $P = [\max(F_o^2,0) + 2F_c^2]/3$. [b] $a = 0.0488$; $b = 0$. [c] $a = 0.0102$; $b = 0$. [d] $a = 0.1654$; $b = 0$.

(d,p) basis set are required in order to better describe possible weak interactions with the metal. The analysis of the electron density was performed with the AIM2000 Release 1 package.[61] Natural bond orbital analyses were performed with the NBO 3.1 program incorporated in the Gaussian package.[62] Molecular orbital diagrams were generated with the MOLDEN program.[63] All the calculations were performed with the Gaussian 01 program suite.[64] Wiberg bond indexes[65] were calculated with the NBO 3.1 program, and Mayer indexes,[66] with the BORDER program.[67] In the case of complexes **2** and **3**, calculations were also made using the Stuttgart/Dresden (SDD)[68] basis set for the molybdenum atoms along with the G-311+(d,p) basis set for the remaining atoms, in order to obtain better quality wavefunctions to submit to the AIM analysis. However, the resulting topologies were essentially identical to those obtained with the LANL2DZ basis set (and no BCP between Mo and H atoms were located either), with the electron densities at the BCP's involving Mo atoms being less than 0.01 e Å^{-3} higher.

X-ray Structure Determination for Compounds 2−4. Full crystallographic data for the title compounds are given in the CIF file format in the Supporting Information, while Table 7 collects the most relevant crystal data for these structural studies. Single-crystal data were collected with a Philips PW 1100 diffractometer (Mo Kα; $\lambda = 0.710\,73$ Å) for **2** and **3** and with a Bruker AXS Smart 1000 area detector diffractometer (Mo Kα; $\lambda = 0.710\,73$ Å) for **4**. Cell constants were obtained from a least-squares refinement of the setting angles of 24 randomly distributed and carefully centered reflections ($10.07 < 2\theta < 19.72$, **2**; $5.02 < 2\theta < 14.61$, **3**) and by a least-squares refinement of 9779 reflections ($2.64 < 2\theta < 27.05$, **4**). No crystal decay was observed for all compounds, and an absorption correction using the program SADABS[69] was applied for **4** (minimum and maximum. transmission factors: 0.679, 1.000). The structures were solved by direct methods (SIR97)[70] and refined with full-matrix least-squares (SHELXL-97),[71] using the Wingx software package.[72] The bridging carbon atom of **2** was statically disordered in two positions, which were refined isotropically with a site occupancy factor of 0.5 each. The H atoms of these two carbon atoms were located from the difference Fourier map, and the H atom positions were refined with the C−H distance restraint of 0.96 Å. The remaining atoms were refined anisotropically. For **3**, non-hydrogen atoms were refined anisotropically and the hydrogen atoms attached to the bridging carbon atom were found from the difference Fourier map and freely refined. The remaining hydrogen atoms were placed at their

(61) (a) http://gauss.fh-bielefeld.de/aim2000. (b) Boegler-König, F.; Schönbohm, J.; Bayles, D. *J. Comput. Chem.* **2001**, *22*, 545−559.
(62) Glendening, E. D.; Reed, A. E.; Carpenter, J. E.; Weinhold, F. NBO version 3.1.
(63) Schaftenaar, G.; Noordik, J. H. *J. Comput.-Aided Mol. Des.* **2000**, *14*, 123.
(64) Frisch, M. J.; Trucks, G. W.; Schlegel, H. B.; Scuseria, G. E.; Robb, M. A.; Cheeseman, J. R.; Montgomery, J. A., Jr.; Vreven, T.; Kudin, K. N.; Burant, J. C.; Millam, J. M.; Iyengar, S. S.; Tomasi, J.; Barone, V.; Mennucci, B.; Cossi, M.; Scalmani, G.; Rega, N.; Petersson, G. A.; Nakatsuji, H.; Hada, M.; Ehara, M.; Toyota, K.; Fukuda, R.; Hasegawa, J.; Ishida, M.; Nakajima, T.; Honda, Y.; Kitao, O.; Nakai, H.; Klene, M.; Li, X.; Knox, J. E.; Hratchian, H. P.; Cross, J. B.; Bakken, V.; Adamo, C.; Jaramillo, J.; Gomperts, R.; Stratmann, R. E.; Yazyev, O.; Austin, A. J.; Cammi, R.; Pomelli, C.; Ochterski, J. W.; Ayala, P. Y.; Morokuma, K.; Voth, G. A.; Salvador, P.; Dannenberg, J. J.; Zakrzewski, V. G.; Dapprich, S.; Daniels, A. D.; Strain, M. C.; Farkas, O.; Malick, D. K.; Rabuck, A. D.; Raghavachari, K.; Foresman, J. B.; Ortiz, J. V.; Cui, Q.; Baboul, A. G.; Clifford, S.; Cioslowski, J.; Stefanov, B. B.; Liu, G.; Liashenko, A.; Piskorz, P.; Komaromi, I.; Martin, R. L.; Fox, D. J.; Keith, T.; Al-Laham, M. A.; Peng, C. Y.; Nanayakkara, A.; Challacombe, M.; Gill, P. M. W.; Johnson, B.; Chen, W.; Wong, M. W.; Gonzalez, C.; Pople, J. A. *Gaussian 03*, Revision B.02; Gaussian: Wallingford, CT, 2004.
(65) Wiberg, K. *Tetrahedron* **1968**, *24*, 1083.
(66) Mayer, I. *Chem. Phys. Lett.* **1983**, *97*, 270.
(67) Mayer, I. *BORDER*, Version 1.0; Chemical Research Center, Hungarian Academy of Sciences: Budapest, Hungary, 2005.
(68) Andrae, D.; Haeussermann, U.; Dolg, M.; Stoll, H.; Preuss, H. *Theor. Chim. Acta* **1990**, *77*, 123.
(69) Sheldrick, G. M. *SADABS, Program for Empirical Absorption Correction*; University of Göttingen: Göttingen, Germany, 1996.
(70) Altomare, A.; Burla, M. C.; Camalli, M.; Cascarano, G. L.; Giacovazzo, C.; Guagliardi, A.; Moliterni, A. G. G.; Polidori, G.; Spagna, R. *J. Appl. Crystallogr.* **1999**, *32*, 115.
(71) Sheldrick, G. M. *SHELX97*. Programs for Crystal Structure Analysis (1997) (Release 97−2); University of Göttingen: Göttingen, Germany.
(72) Farrugia, L. J. *J. Appl. Crystallogr.* **1999**, *32*, 837.

calculated positions. In **4** there is a static disorder involving the bridging phenyl group and possibly a chlorine atom; this presumes the cocrystallization of $[Mo_2Cp_2(\mu\text{-}Ph)(\mu\text{-}PCy_2)(CO)_2]$ and $[Mo_2Cp_2(\mu\text{-}Cl)(\mu\text{-}PCy_2)(CO)_2]$, the latter possibly being formed accidentally to a small extent during the chromatographic workup of the sample of **3** used to grow the crystals used, which were repeatedly of very poor quality. The site occupancy factors for the two units were refined as 0.75 and 0.25, respectively. Due to the poor quality of the data set, the Cp and Ph rings were refined isotropically and the hydrogen atoms were placed at their calculated positions. Graphical material was prepared with the ORTEP3 for Windows program.[73]

(73) Farrugia, L. J. *J. Appl. Crystallogr.* **1997**, *30*, 565.

Acknowledgment. We thank one of the reviewers for providing relevant suggestions to improve the refinement of the crystal structure of compound **2**. We also thank the MEC of Spain for a grant (to A.R.) and financial support (Project BQU2003-05478).

Supporting Information Available: Crystallographic data for the structural analysis of compounds **2**−**4** (CIF) and atomic coordinates calculated for **A** and compounds **1**−**4** (xyz). This material is available free of charge via the Internet at http://pubs.acs.org.

OM7007265